THE UNIVERSITY OF WESTERN ONTARIO
DEPARTMENT OF CIVIL AND
ENVIRONMENTAL ENGINEERING

Water Resources Research Report

Development of Nonstationary Rainfall Intensity Duration Frequency Curves for Future Climate Conditions

By:
Daniele Feitoza Silva
and
Slobodan P. Simonovic

Report No: 106
Date: April 2020

ISBN: (print) 978-0-7714-3137-1; (online) 978-0-7714-3138-8

DEVELOPMENT OF NON-STATIONARY RAINFALL INTENSITY DURATION FREQUENCY CURVES FOR FUTURE CLIMATE CONDITIONS

Western
UNIVERSITY · CANADA

By

Daniele Feitoza Silva

and

Slobodan P. Simonovic

Department of Civil and Environmental Engineering
Western University, Canada

April, 2020

Executive Summary

Cities worldwide are facing the impacts of climate change, and the integrity and management of water infrastructure is an important aspect to ensure safety and well-being of population. One way to address these changes is incorporating them into the urban design and planning, particularly in terms of extreme precipitation events. Intensity-Duration-Frequency (IDF) curves are the most commonly used tool for this purpose. Among other assumptions, those curves are generated under stationarity assumption. This assumption does not hold on under climate change which is already changing rainfall patterns or/and will change them in the future. This report proposes an innovative methodology which aims to include not stationary (nonstationary) behavior into the development of future IDFs. Our methodology includes (i) fitting Generalized Extreme Value (GEV) model parameter combinations with time as covariate, (ii) testing data statistics, (iii) downscaling data in time and space, and (iii) optimizing IDFs equation parameters. The open access RStudio software was used to implement the methodology at six gauging stations across Canada. Only, London gauging station (Ontario, Canada) is used in this report to illustrate the application of the proposed methodology.

Table of Contents

List of Figures

List of Tables

1 Introduction

Changes in climate conditions observed over the last few decades are considered to be the cause of change in patterns of extreme precipitation events. Observations suggest an increase in global temperature, which increases the amount of water vapor in the atmosphere and influences hydro-climatic processes, affecting the magnitude and frequency of extreme precipitation events in most of Canada (IPCC, 2014). In cities, impacts of climate change increases disaster risk since they are not prepared for changing conditions. Incorporating expected changes in planning, design, operation and maintenance of water infrastructure would reduce unseen future uncertainties that may result from increase in frequency and magnitude of extreme rainfall events.

Traditional methodologies based on local Intensity-Duration-Frequency (IDF) curves are commonly used for stormwater management and infrastructure design activities. Reliable rainfall intensity estimates are necessary for hydrologic analyses, planning, management and design of water infrastructure systems. Information from IDF curves are used to describe the frequency of extreme rainfall events of various intensities and durations. The rainfall IDF curve is one of the most commonly used tools in urban drainage engineering, and application of IDF curves for a variety of water management applications has been increasing (CSA, 2010). IDF curves are typically developed by fitting a theoretical probability distribution to an annual maximum precipitation (AMP) time series. IDF curves generation is based on following assumptions: 1) data homogeneity, which ensures data is provided by the same gauging station and is obtained in the same way; 2) data randomness, which ensures the nature of data; 3) data independence, which means a particular annual maxima does not influence the annual maxima in the following year; and 4) data stationarity, which means that the statistical properties of a process generating a time series do not change over time. AMP data are fitted using extreme value distributions like Gumbel, Generalized Extreme Value (GEV), Log-Pearson, Log-Normal, among others. IDF curves provide precipitation accumulation depths for various return periods (T) and different durations, usually, 5, 10, 15, 30 minutes, 1, 2, 6, 12, 18 and 24 hours. Durations exceeding 24 hours may also be used, depending on the application of IDF curves. Hydrologic design of storm sewers, culverts, detention basins and other elements of storm water management systems is typically performed based on specified design storms derived from IDF curves (Solaiman and Simonovic, 2010; Peck et al., 2012).

Under a changing climate, approaches to water resources management have improved in order to quantify climate change impacts and reduce risks. For this, two points need attention. First, the increase in extremes events is expected and stationarity assumption may not be valid anymore, and infrastructure systems capacity to deliver a required service may be underestimated. Non-stationary behavior implies existence of a trend in the probability distribution parameter value(s) associated with covariate(s) (see Figure 1 for illustration of the difference between stationary and nonstationary IDF relationship). Therefore, it is necessary to investigate non-stationarity in historic data and find a way to translate this information into the IDF development. A covariate is a possible predictive or explanatory variable of the dependent variable and may include time (Sugahara et al., 2009; Cheng et al., 2014; Cheng and AghaKouchak, 2014) or any variable associated with an independent physical process, i.e. climate variables (Mondal and Mujumdar, 2015; Agilan and Umamahesh, 2015; 2017; Ouarda et al., 2018).

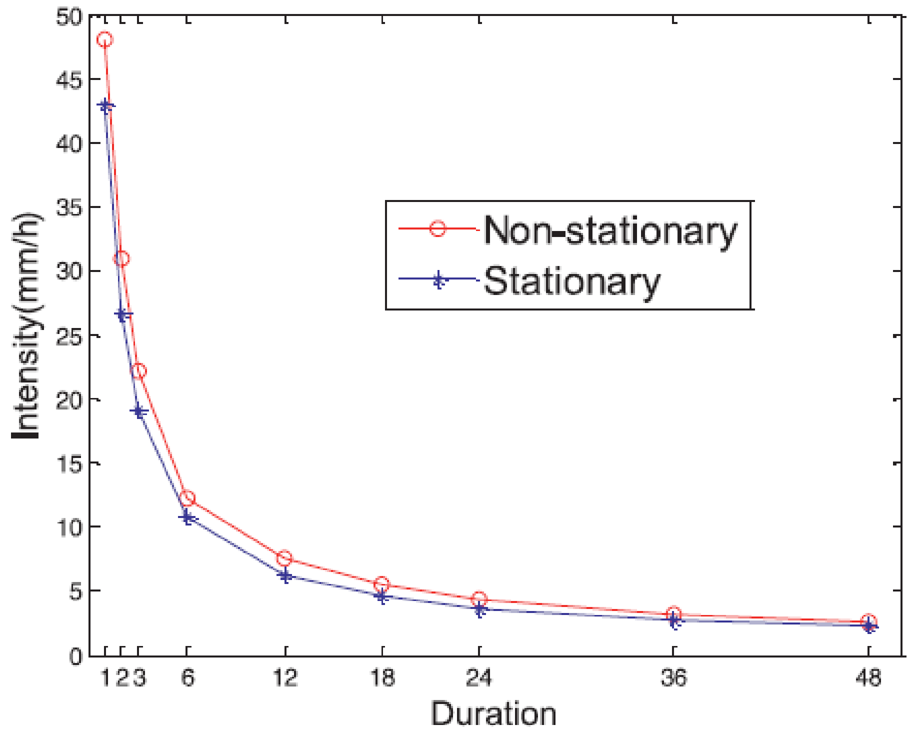

Figure 1. Illustration of stationary and nonstationary IDF relationships. Source (Agilan and Umamahesh, 2017)

In this study, we assess the effect of non-stationarity on: (i) historical IDF curves developed using observed data; and (ii) IDF curves updated for future conditions based on climate change projections, by considering time as a covariate. The content of this report includes the methodology for development of non-stationary IDFs, its implementation and an illustrative example. All necessary information is provided in the report appendixes.

2 Methodology for the Development of Non-stationary IDFs

The methodology adopted for the development of non-stationary IDFs includes: (i) Statistical analysis for fitting GEV distribution using the Maximum Likelihood method; (ii) Statistical analysis for identifying non-stationarity; defining the best model; and assessing the statistical significance of the non-stationary model in comparison to the stationary model; and (iii) IDF updating algorithms to address the impacts of climate change for gauged locations. The next section presents the algorithm, and its implementation with the IDF_CC tool for updating IDF curves (Schardong, et al, 2020) is presented.

GEV probability distribution is adopted to estimate parameters. This distribution has a wide variety of applications for estimating extreme values of given data sets and is commonly used in hydrologic applications. It is used to generate the extreme precipitation for various return periods and different durations. A corrected Akaike Information Criteria (AICc) is adopted to identify the presence of non-stationarity in parameter(s) distribution, and also define the best GEV model among several non-stationary GEV models and one stationary GEV model. The significance of the best non-stationary model against the stationary model is checked by the Likelihood ratio test, through which the negative log-likelihood of both models is compared to test the null hypothesis of no trend in a parameter.

2.1 Generalized Extreme Value (GEV) Distribution

The GEV distribution is a family of continuous probability distributions that combines the three asymptotic extreme value distributions into a single one: Gumbel (EV1), Fréchet (EV2) and Weibull (EV3). The GEV distribution is flexible for modeling different behavior of extremes with three distribution parameters: location, scale and shape (Cheng et al., 2014). The location parameter describes the shift of a distribution in each direction on the horizontal axis. The scale parameter describes how spread out distribution is, and defines where the bulk of the distribution lies. As the scale parameter increases, the distribution becomes more spread out. The shape parameter affects the characteristics of distribution tail. The shape parameter is derived from skewness, as it represents where most of the data lies, which create the tail(s) of the distribution. The value of shape parameter $\xi = 0$, indicates the light tale EV1 (Gumbel) distribution. Value of $\xi > 0$ indicates EV2 (Fréchet), and $\xi < 0$ the EV3 (Weibull). The Fréchet type has a longer (heavy) upper tail than the Gumbel distribution and the Weibull has a short tail (Overeem et al., 2007; Millington et al., 2011).

A common statistical procedure for estimating distribution parameters is the use of a maximum likelihood estimator, since this method can be easily extended to the non-stationary case. Non-stationarity is introduced by expressing one or more of the parameters of the GEV as a function of time, as $\mu(t)$, $\sigma(t)$ and $\xi(t)$, t = 1,2,… (Coles, 2001; Katz, 2013).

The GEV cumulative distribution function F(x) is given by Eq. 1 for $\xi \neq 0$.

$$F(x) = exp\left\{-\left[1 + \frac{\xi(t)(x-\mu(t))}{\sigma(t)}\right]^{-1/\xi(t)}\right\}, \text{ for } \xi \neq 0 \quad (1)$$

with μ as location parameter, σ as scale parameter and ξ as the shape parameter of the distribution.

In this study, besides a stationary GEV model (Table 1 – Type I), we have also considered eight combinations of GEV parameters (Table 1 – Type II to IX), by assuming linear and quadratic trends to location parameter, linear and exponential trend to scale parameter, and their different combinations.

Table 1. GEV models adopted

Type	Parameters combination
I	$\mu(t) = \mu$ $\sigma(t) = \sigma$ $\xi(t) = \xi$
II	$\mu(t) = \mu0 + \mu1 * \mathrm{t}$ $\sigma(t) = \sigma$ $\xi(t) = \xi$
III	$\mu(t) = \mu0 + \mu1 * \mathrm{t}$ $\sigma(t) = \sigma0 + \sigma1 * t$ $\xi(t) = \xi$
IV	$\mu(t) = \mu0 + \mu1 * \mathrm{t}$ $\sigma(t) = \exp(\sigma0 + \sigma1 * t)$ $\xi(t) = \xi$
V	$\mu(t) = \mu$ $\sigma(t) = \sigma0 + \sigma1 * t$ $\xi(t) = \xi$
VI	$\mu(t) = \mu$ $\sigma(t) = \exp(\sigma0 + \sigma1 * t)$ $\xi(t) = \xi$
VII	$\mu(t) = \mu0 + \mu1 * \mathrm{t} + \mu2 * t^2$ $\sigma(t) = \sigma0$ $\xi(t) = \xi$
VIII	$\mu(t) = \mu0 + \mu1 * \mathrm{t} + \mu2 * t^2$ $\sigma(t) = \sigma0 + \sigma1 * t$ $\xi(t) = \xi$
IX	$\mu(t) = \mu0 + \mu1 * \mathrm{t} + \mu2 * t^2$ $\sigma(t) = \exp(\sigma0 + \sigma1 * t)$ $\xi(t) = \xi$

Considering a particular duration of rainfall data, let the values X = $x_1, x_2, \ldots, x_n$ be the n years of annual maximum series. For the stationary case, the log likelihood derived from Eq. 1 is given as:

For $\xi \neq 0$ and $1 + \xi\left(\frac{x_i-\mu}{\sigma}\right) > 0$,

$$\log\mathrm{L}(\mu, \sigma, \xi|X) = -n\log\sigma - \left(1 + \frac{1}{\xi}\right)\sum_{i=1}^{n} \log\left[1 + \xi(\frac{x_i-\mu}{\sigma})\right] - \sum_{i=1}^{n}\left[1 + \xi(\frac{x_i-\mu}{\sigma})\right]^{-1/\xi} \quad (2)$$

The maximum likelihood estimates (MLEs) are those values of the parameters that maximize the likelihood function. Instead of maximization, it is more convenient to minimize the negative log likelihood function (-logL – Eq. 2). With this formulation, the extension to the non-stationary case, in which the parameters of the GEV distribution depend on time t (Katz, 2013). To obtain the parameters of extremal distributions as the GEV by minimizing the negative log likelihood function, requires iterative numerical procedure.

2.2 Identification of the best GEV model

After non-stationary models' development, it is important to identify which model better represents the original data. To select the best model, we use the corrected Akaike Information Criteria (AICc), which penalizes the minimized negative log likelihood for the number of parameters estimated, (Katz, 2013). According to Sugahara et al. (2009), AICc is recommended in practical applications because it outperforms the original AIC and helps to avoid over-fitting the data.

From a collection of nested candidate models, AIC selects the model that minimizes the quantity:

$$AIC(k) = 2 * nllh(k) + 2k \qquad (3)$$

where $nllh = -\log L$, is the minimized negative log likelihood function; and *k* is the number of parameters of the specific model.

For a candidate model with k parameters, which has a sample size of *n*, then the AICc of the model is as follows:

$$AICc(k) = AIC(k) + \frac{2k(k+1)}{n-k-1} \qquad (4)$$

The rescaled form of AICc, Δ_i is used to rank the GEV models as follows:

$$\Delta_i = AICc - \min(AICc) \qquad (5)$$

where *min*$(AICc)$ is the smallest $AICc$ among all the models. The model which has Δ_i value zero is the best model and the models having $\Delta_i \leq 2$ are considerable reasonable good choices (Burnham and Anderson, 2004).

2.3 Significance of the best GEV model

The statistical significance of the best non-stationary model against the stationary one can be provided by the Likelihood Ratio test, by assessing the statistical significance of the trend parameter in the non-stationary model. The test of the null hypothesis of no trend in a parameter value can be performed by comparing the minimized negative log likelihood function of two competing models (one as the stationary and other as the best non-stationary, as explained in section 3.2) (Katz, 2013). That is, a comparison of:

$nllh_s$ x $nllh_{ns}$

where $nllh_s$ is the negative log likelihood of the stationary model, and $nllh_{ns}$ is the negative log likelihood of the best non-stationary model.

Under a null hypothesis of no trend, the likelihood ratio test statistic, based on twice the difference between $nllh_s$ and $nllh_{ns}$, has an approximate chi squared distribution with degree of freedom denoted as the difference between a number of parameters (Katz, 2013). The test is based on:

$$2[nllh_s - nllh_{ns}] \sim \chi^2 \quad (6)$$

The statistical significance of the best non-stationary model, when compared to the stationary model, can be measured from the *p*-value of Chi-square distribution (Agilan and Umamanesh, 2017). Once the *p*-value < 0.05 (considering 95% confidence level), the best non-stationary model presents statistical significance in comparison to the stationary model.

2.4 Sub-daily annual maximums for future

The development of IDFs under a changing climate follows the Equidistant Quantile Matching procedure (Srivastav et al., 2014) implemented by the IDF_CC tool (Schardong et al, 2020). Future rainfall data is obtained based on GCMs and downscaling techniques to capture (i) the changes in the GCM daily data between the baseline period and the future period, and (ii) the relationship between observed sub-daily data and GCM daily data for the baseline period. Presence of non-stationarity is possible here too. The flow chart of the revised EQM methodology to include non-stationarity is shown in Figure 2.

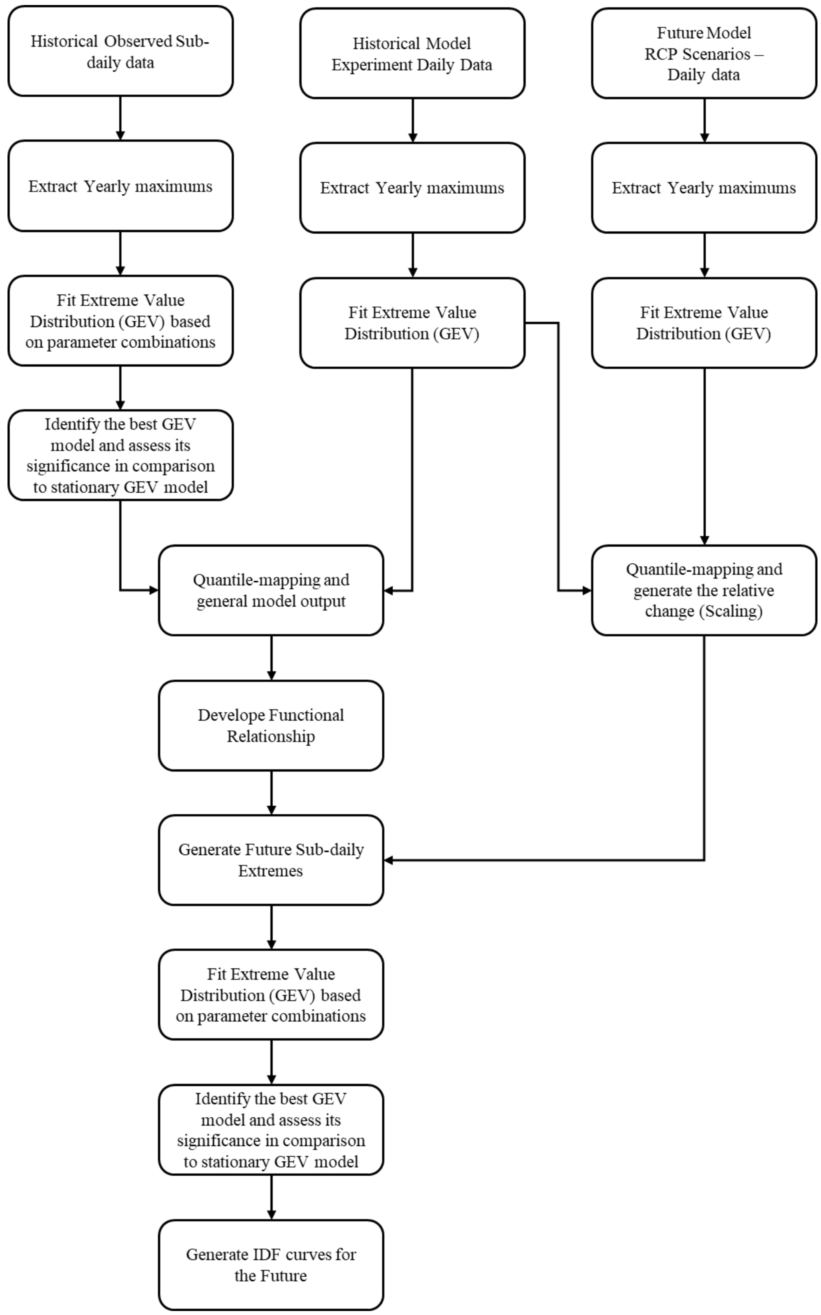

Figure 2. Revised Equidistance Quantile Matching method for generating IDF curves under climate change considering a non-stationary behavior

The following section presents the revised EQM method for updating the IDF curves considering a non-stationary behavior. The following notation is used in the descriptions of the updated EQM steps: x, stands for the annual maximum precipitation, j is the subscript for 5min, 10min, 15min, 30min, 1hr, 2hr, 6hr, 12hr, 24hr sub-daily durations, o the observed historical series, h historical simulation period (base-line for model data), m model (downscaled GCMs), f the sub/superscript for the future projected series, F the CDF of the fitted probability GEV distribution, and F^{-1} the inverse CDF. The steps involved in the revised algorithm are as follows:

(i) Extract sub-daily maximums $x_{j,o,h}$ from the observed data at a given location (i.e., maximums of 5min, 10min, 15min, 30min, 1hr, 2hr, 6hr, 12hr, 24hr precipitation data).
(ii) Extract daily maximums for the historical baseline period from the selected GCMs, $x_{m,h}$.
(iii) Fit the GEV probability distribution to time series extracted in (i) for each sub-daily duration, $F_{j,o,h}$, for the nine parameters combinations as presented in Table 1.
(iv) Identify the best GEV model among the nine GEV models fitted in (iii) by applying the corrected Akaike Information Criteria (AICc).
(v) If a non-stationary model is identified as better than the stationary, assess its significance using the Likelihood Ratio test.
(vi) Fit the GEV probability distribution to time series extracted in step (ii), $F_{m,h}$.
(vii) When a non-stationary GEV model is detected, the parameter(s) of the sub-daily series is(are) calculated based on the 95 percentiles of the trending parameter value. The cumulative probability distribution of the GCM ($F_{m,h}$) and the fit parameters of the sub-daily series ($\theta_{j,o,h}$) are equated to establish a statistical relationship in the following form:

$$\hat{x}_{j,o,h} = \frac{a_j + x_{m,h}}{b_j + c_j x_{m,h}} + \frac{d_j}{x_{m,h}} \tag{7}$$

where $\hat{x}_{j,o,h}$ corresponds to the AMP quantiles at the station scale and a_j, b_j, c_j and d_j, are the adjusted coefficients of the equation for each sub-daily duration *j*. A Differential Evolution (DE) optimization algorithm is used to fit the coefficientsa_j, b_j, c_j and d_j.

(viii) Extract daily maximums from the RCP scenarios (i.e., RCP 2.6, RCP 4.5, RCP 8.5) for the selected GCM model, $x_{m,f}$.
(ix) For each future precipitation series$x_{m,f}$, calculate the nonexceedance probability $\tau_{m,f}$ from the fitted GEV, $F_{m,f}$. Find the corresponding quantile ($\hat{x}_{m,h}$) at the GCM historical baseline by entering the value of $\tau_{m,f}$ in the inverse CDF ${F^{-1}}_{m,f}$. This is a scaling step introduced to incorporate the future projections in the updated IDF and uses the concepts of quantile delta mapping (Olsson et al., 2009; and Cannon et al., 2015). The relative change Δ_m, is calculated using Eq. 10:

$$\tau_{m,f} = F_{m,f}(x_{m,f}) \tag{8}$$

$$\hat{x}_{m,h} = {F^{-1}}_{m,h}(\tau_{m,f}) \tag{9}$$

$$\Delta_m = \frac{x_{m,f}}{\hat{x}_{m,h}} \tag{10}$$

To generate the projected future maximum sub-daily series at the station scale ($x_{j,o,h}^f$), use Eq. 7 by replacing $x_{m,h}$ to $\hat{x}_{m,h}$ and multiplying by the relative change Δ_m from Eq. 10.

$$x_{j,o,h}^f = \Delta_m . \hat{x}_{j,o,h} \tag{11}$$

(x) Consider the effects of non-stationarity in the projected future maximum sub-daily data by applying steps (iv) and (v) when this behavior is confirmed.

2.5 IDF Curves

IDF curves are adjusted equations based on the estimated values T-year return levels. The inverse distribution function or quantile function is given by Eq. 12 for $\xi \neq 0$.

$$Q(x) = \mu(t) - \frac{\sigma(t)}{\xi(t)}\{[1 - (-\ln(1 - 1/T)]^{-\xi(t)}\}, \text{ for } \xi \neq 0 \tag{12}$$

where: T – return period (years).

The return levels are then translated in intensities, for each duration and return period. A curve can be adjusted using precipitation intensity results and by Differential Evolutionary optimization. The IDF relationship is obtained as follows:

$$i(T) = A(t + to)^B \tag{13}$$

where: *A, B*, and to are adjusted coefficients; and *t* is duration (h).

3 Implementation of the Methodology

This section describes the methodology implementation process used to update IDF curves under non-stationary behaviour at six different locations across Canada.

3.1 Data

For the purpose of this study, the sub-daily rainfall data at six gauging stations are utilized.

Table **2** presents relevant information about selected stations.

Table 2: Stations analyzed in this study

Station (code)	Location	Latitude	Longitude	Period
CALGARY INT'L CS (3031094)	Calgary, AB	114 0' W	51 7' N	1947-2015
HAMILTON RBG CS 6153301	Hamilton, ON	43 17' N	79 55' W	1962-2016
LONDON CS 6144478	London, ON	43 2' N	81 9' W	1943-2016
MONCTON INTL A 8103201	Moncton, NB	46 7' N	64 41' W	1946-2016
VANCOUVER INTL A 1108395	Vancouver, BC	49 11' N	123 11' W	1953-2017
WINNIPEG A CS 502S001	Winnipeg, MB	49 55' N	97 15' W	1944-2016

GCMs model data were obtained for 24 climate models available from the IDF_CC tool (list of the models used is in Appendix A) for three RCP scenarios (i.e., RCP 2.6, RCP 4.5, and RCP 8.5). However, in this report only calculation for the City of London gauging station is used as an illustrative example (presented in Section 4 of this report).

3.2 RStudio Software

Estimation of the GEV model parameters requires iterative numerical procedure. For this study the RStudio programming is used, since it provides packages and functions necessary for estimation of GEV model parameters and identification of trends in them.

RStudio (R Development Core Team, 2011) is a public domain software available under the GNU General Public License, with an integrated development environment for R, a programming language for graphics and statistical analysis. R and its libraries oriented toward data manipulation, statistical analyses and the production of high-quality graphics, can be linked to other software through functions and extension. For this study, some specific functions were used which includes:

- Statistical: RStudio includes packages and coding tools to fit parameter to several distributions, even for nonstationary purposes, and performs statistical tests;
- Optimization: RStudio performs evolutionary global optimization via the Differential Evolution algorithm, used here for downscaling procedures and to fit coefficients.
- Graphics: RStudio supports functions that provide interactive graphics based on different functions.

3.3 GEV model parameters

For the assessment of non-stationary behavior, we used RStudio software, and R packages "extRemes" version 2.0-10 and "ismev" version 1.42, by using *fevd* (Figure 3) or *gev.fit* (Figure 4) functions, respectively (R Development Core Team, 2011; Grilleland, 2018; 2019). Both functions use the form of GEV model described in Coles (2001). The output obtained includes: (i) the fitted GEV parameters for each combination from Table 1; (ii) the value of AIC, which is used to identify the best GEV model; and (iii) the value of the negative log-likelihood, which is used to estimate the significance of the best GEV model.

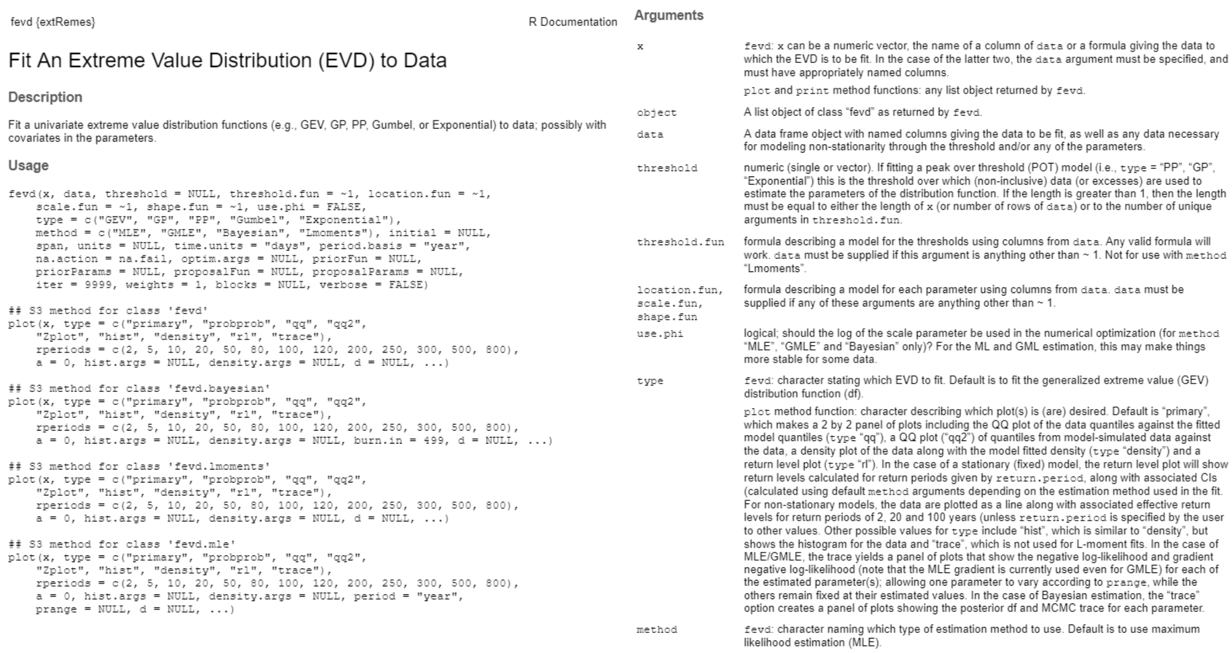

fevd {extRemes} R Documentation

Fit An Extreme Value Distribution (EVD) to Data

Description

Fit a univariate extreme value distribution functions (e.g., GEV, GP, PP, Gumbel, or Exponential) to data; possibly with covariates in the parameters.

Usage

```
fevd(x, data, threshold = NULL, threshold.fun = ~1, location.fun = ~1,
    scale.fun = ~1, shape.fun = ~1, use.phi = FALSE,
    type = c("GEV", "GP", "PP", "Gumbel", "Exponential"),
    method = c("MLE", "GMLE", "Bayesian", "Lmoments"), initial = NULL,
    span, units = NULL, time.units = "days", period.basis = "year",
    na.action = na.fail, optim.args = NULL, priorFun = NULL,
    priorParams = NULL, proposalFun = NULL, proposalParams = NULL,
    iter = 9999, weights = 1, blocks = NULL, verbose = FALSE)

## S3 method for class 'fevd'
plot(x, type = c("primary", "probprob", "qq", "qq2",
    "Zplot", "hist", "density", "rl", "trace"),
    rperiods = c(2, 5, 10, 20, 50, 80, 100, 120, 200, 250, 300, 500, 800),
    a = 0, hist.args = NULL, density.args = NULL, d = NULL, ...)

## S3 method for class 'fevd.bayesian'
plot(x, type = c("primary", "probprob", "qq", "qq2",
    "Zplot", "hist", "density", "rl", "trace"),
    rperiods = c(2, 5, 10, 20, 50, 80, 100, 120, 200, 250, 300, 500, 800),
    a = 0, hist.args = NULL, density.args = NULL, burn.in = 499, d = NULL, ...)

## S3 method for class 'fevd.lmoments'
plot(x, type = c("primary", "probprob", "qq", "qq2",
    "Zplot", "hist", "density", "rl", "trace"),
    rperiods = c(2, 5, 10, 20, 50, 80, 100, 120, 200, 250, 300, 500, 800),
    a = 0, hist.args = NULL, density.args = NULL, d = NULL, ...)

## S3 method for class 'fevd.mle'
plot(x, type = c("primary", "probprob", "qq", "qq2",
    "Zplot", "hist", "density", "rl", "trace"),
    rperiods = c(2, 5, 10, 20, 50, 80, 100, 120, 200, 250, 300, 500, 800),
    a = 0, hist.args = NULL, density.args = NULL, period = "year",
    prange = NULL, d = NULL, ...)
```

Arguments

`x`	`fevd`: `x` can be a numeric vector, the name of a column of `data` or a formula giving the data to which the EVD is to be fit. In the case of the latter two, the `data` argument must be specified, and must have appropriately named columns. `plot` and `print` method functions: any list object returned by `fevd`.
`object`	A list object of class "fevd" as returned by `fevd`.
`data`	A data frame object with named columns giving the data to be fit, as well as any data necessary for modeling non-stationarity through the threshold and/or any of the parameters.
`threshold`	numeric (single or vector). If fitting a peak over threshold (POT) model (i.e., `type` = "PP", "GP", "Exponential") this is the threshold over which (non-inclusive) data (or excesses) are used to estimate the parameters of the distribution function. If the length is greater than 1, then the length must be equal to either the length of `x` (or number of rows of `data`) or to the number of unique arguments in `threshold.fun`.
`threshold.fun`	formula describing a model for the thresholds using columns from `data`. Any valid formula will work. `data` must be supplied if this argument is anything other than ~ 1. Not for use with `method` "Lmoments".
`location.fun, scale.fun, shape.fun`	formula describing a model for each parameter using columns from `data`. `data` must be supplied if any of these arguments are anything other than ~ 1.
`use.phi`	logical; should the log of the scale parameter be used in the numerical optimization (for `method` "MLE", "GMLE" and "Bayesian" only)? For the ML and GML estimation, this may make things more stable for some data.
`type`	`fevd`: character stating which EVD to fit. Default is to fit the generalized extreme value (GEV) distribution function (df). `plot` method function: character describing which plot(s) is (are) desired. Default is "primary", which makes a 2 by 2 panel of plots including the QQ plot of the data quantiles against the fitted model quantiles (`type` "qq"), a QQ plot ("qq2") of quantiles from model-simulated data against the data, a density plot of the data along with the model fitted density (`type` "density") and a return level plot (`type` "rl"). In the case of a stationary (fixed) model, the return level plot will show return levels calculated for return periods given by `return.period`, along with associated CIs (calculated using default `method` arguments depending on the estimation method used in the fit. For non-stationary models, the data are plotted as a line along with associated effective return levels for return periods of 2, 20 and 100 years (unless `return.period` is specified by the user to other values. Other possible values for `type` include "hist", which is similar to "density", but shows the histogram for the data and "trace", which is not used for L-moment fits. In the case of MLE/GMLE, the trace yields a panel of plots that show the negative log-likelihood and gradient negative log-likelihood (note that the MLE gradient is currently used even for GMLE) for each of the estimated parameter(s); allowing one parameter to vary according to `prange`, while the others remain fixed at their estimated values. In the case of Bayesian estimation, the "trace" option creates a panel of plots showing the posterior df and MCMC trace for each parameter.
`method`	`fevd`: character naming which type of estimation method to use. Default is to use maximum likelihood estimation (MLE).

Figure 3. *fevd* documentation for RStudio

gev.fit {ismev} R Documentation

Maximum-likelihood Fitting of the GEV Distribution

Description

Maximum-likelihood fitting for the generalized extreme value distribution, including generalized linear modelling of each parameter.

Usage

```
gev.fit(xdat, ydat = NULL, mul = NULL, sigl = NULL, shl = NULL,
    mulink = identity, siglink = identity, shlink = identity,
    muinit = NULL, siginit = NULL, shinit = NULL,
    show = TRUE, method = "Nelder-Mead", maxit = 10000, ...)
```

Arguments

`xdat`	A numeric vector of data to be fitted.
`ydat`	A matrix of covariates for generalized linear modelling of the parameters (or `NULL` (the default) for stationary fitting). The number of rows should be the same as the length of `xdat`.
`mul, sigl, shl`	Numeric vectors of integers, giving the columns of `ydat` that contain covariates for generalized linear modelling of the location, scale and shape parameters repectively (or `NULL` (the default) if the corresponding parameter is stationary).
`mulink, siglink, shlink`	Inverse link functions for generalized linear modelling of the location, scale and shape parameters repectively.
`muinit, siginit, shinit`	numeric of length equal to total number of parameters used to model the location, scale or shape parameter(s), resp. See Details section for default (NULL) initial values.
`show`	Logical; if `TRUE` (the default), print details of the fit.
`method`	The optimization method (see `optim` for details).
`maxit`	The maximum number of iterations.
`...`	Other control parameters for the optimization. These are passed to components of the `control` argument of `optim`.

Figure 4. *gev.fit* documentation for RStudio

3.4 Identification of the best GEV model

Using AIC results, *k* as the number of model parameters, and *n* as the data length, the best GEV model is identified by using Equations 4 and 5. The procedure can be implemented using RStudio by programming the appropriate equation or simply using Excel environment.

3.5 Significance of the best GEV model

Once the best non-stationary GEV model is identified, it is necessary to test its significance. Using *nllh* results and the Chi-Square distribution table, the Equation 6 is applied to calculate test statistics. Otherwise, the function *lr.test* (Figure 5) in RStudio can calculate *p*-value. In presented work $\alpha = 0.05$ (significance value) is used. If *p*-value is lower than 0.05, the null hypothesis that there is no trend in GEV parameters model type is rejected.

lr.test {extRemes} R Documentation

Likelihood-Ratio Test

Description

Conduct the likelihood-ratio test for two nested extreme value distribution models.

Usage

```
lr.test(x, y, alpha = 0.05, df = 1, ...)
```

Arguments

`x, y`	Each can be either an object of class “fevd” (provided the fit method is MLE or GMLE) or a single numeric giving the negative log-likelihod value for each model. `x` should be the model with fewer parameters, but if both `x` and `y` are “fevd” objects, then the order does not matter (it will be determined from which model has more parameters).
`alpha`	single numeric between 0 and 1 giving the significance level for the test.
`df`	single numeric giving the degrees of freedom. If both `x` and `y` are “fevd” objects, then the degrees of freedom will be calculated, and this argument ignored. Otherwise, if either or both of `x` and `y` are single numerics, then it must be provided or the test may be invalid.
`...`	Not used.

Details

When it is desired to incorporate covariates into an extreme value analysis, one method is to incorporate them into the parameters of the extreme value distributions themselves in a regression-like manner (cf. Coles, 2001 ch 6; Reiss and Thomas, 2007 ch 15). In order to justify whether or not inclusion of the covariates into the model is significant or not is to apply the likelihood-ratio test (of course, the test is more general than that, cf. Coles (2001) p 35).

The test is only valid for comparing nested models. That is, the parameters of one model must be a subset of the parameters of the second model.

Suppose the base model, m0, is nested within the model m1. Let `x` be the negative log-likelihood for m0 and `y` for m1. Then the likelihood-ratio statistic (or deviance statistic) is given by (Coles, 2001, p 35; Reiss and Thomas, 2007, p 118):

D = -2*(`y` - `x`).

Letting c.alpha be the (1 - alpha) quantile of the chi-square distribution with degrees of freedom equal to the difference in the number of model parameters, the null hypothesis that D = 0 is rejected if D > c.alpha (i.e., in favor of model m1).

Figure 5. *lr.test* documentation for RStudio

3.6 Return level estimation

Return level is also estimated using RStudio programming. *erlevd* function (Figure 6) is capable to calculate return level for a given return period. In the case of a non-stationary model with time as covariate, *erlevd* can calculate a return level for each value of the covariate(s) used to fit the model to data. However, for development of IDF curves, we used the 95th percentile of return level value, which is equal to calculate 95th percentiles of parameters and applied to return level equation.

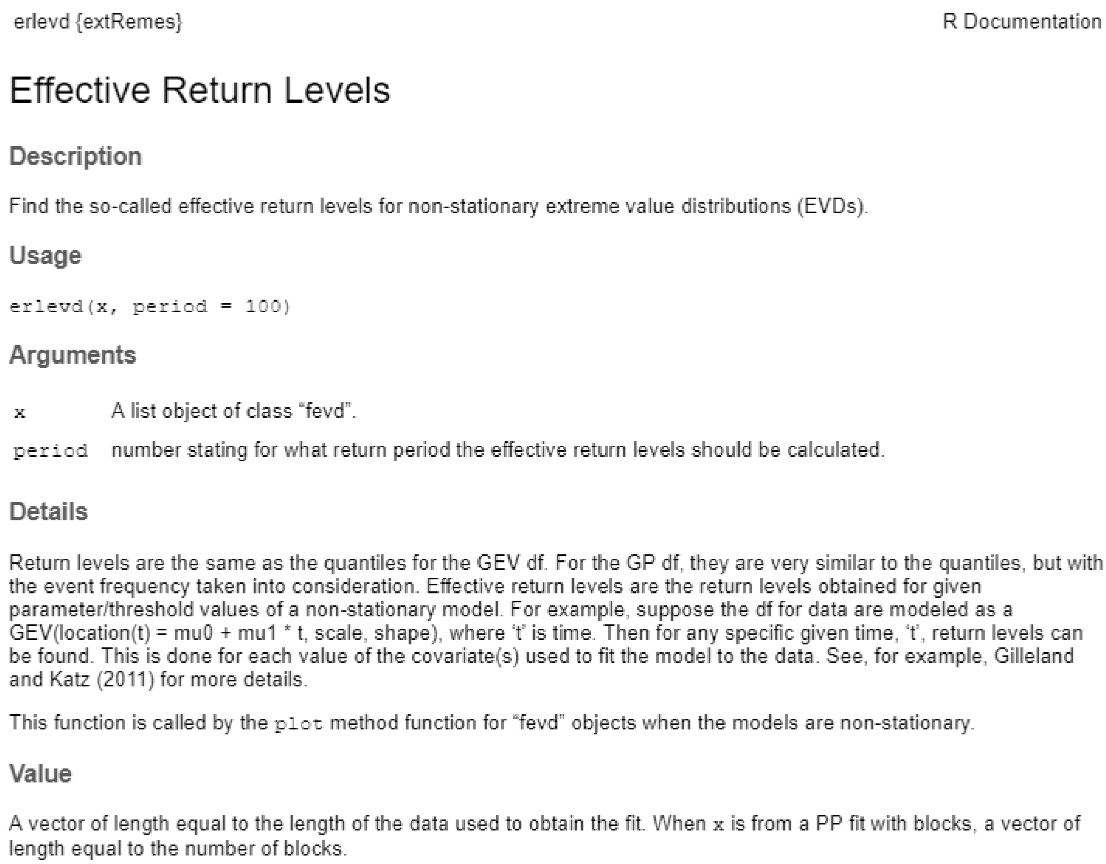
erlevd {extRemes} R Documentation

Effective Return Levels

Description

Find the so-called effective return levels for non-stationary extreme value distributions (EVDs).

Usage

```
erlevd(x, period = 100)
```

Arguments

`x`	A list object of class "fevd".
`period`	number stating for what return period the effective return levels should be calculated.

Details

Return levels are the same as the quantiles for the GEV df. For the GP df, they are very similar to the quantiles, but with the event frequency taken into consideration. Effective return levels are the return levels obtained for given parameter/threshold values of a non-stationary model. For example, suppose the df for data are modeled as a GEV(location(t) = mu0 + mu1 * t, scale, shape), where 't' is time. Then for any specific given time, 't', return levels can be found. This is done for each value of the covariate(s) used to fit the model to the data. See, for example, Gilleland and Katz (2011) for more details.

This function is called by the `plot` method function for "fevd" objects when the models are non-stationary.

Value

A vector of length equal to the length of the data used to obtain the fit. When `x` is from a PP fit with blocks, a vector of length equal to the number of blocks.

Figure 6. *erlevd* documentation for RStudio

3.7 Sub-daily future data

Sub-daily future analysis is performed following algorithm steps presented in Section 2.4. The implementation is made in RStudio environment, by using presented functions, in order to estimate and test GEV parameters for different time-covariant combinations.

A relationship between GCM model daily data and sub-daily observed data, and adjustments of coefficients according to Equation 7, are developed using the package "DEoptim" version 2.2-4 (Ardia et al., 2016), through *DEoptim* function (Figure 7). This function performs optimization via the Differential Evolution algorithm. We used the Ordinary Least Squares (OLS) method as the objective function to be optimized (minimized) in order to obtain the optimal set of coefficients.

3.8 IDF curves

IDF curves are obtained by adjusting precipitation intensities estimated by *erlevd* function. The curve coefficients are obtained using Equation 13, for each return period. *DEoptim* and OLS function are used to adjust those coefficients.

DEoptim {DEoptim} R Documentation

Differential Evolution Optimization

Description

Performs evolutionary global optimization via the Differential Evolution algorithm.

Usage

```
DEoptim(fn, lower, upper, control = DEoptim.control(), ..., fnMap=NULL)
```

Arguments

`fn`	the function to be optimized (minimized). The function should have as its first argument the vector of real-valued parameters to optimize, and return a scalar real result. `NA` and `NaN` values are not allowed.
`lower, upper`	two vectors specifying scalar real lower and upper bounds on each parameter to be optimized, so that the i-th element of `lower` and `upper` applies to the i-th parameter. The implementation searches between `lower` and `upper` for the global optimum (minimum) of `fn`.
`control`	a list of control parameters; see `DEoptim.control`.
`fnMap`	an optional function that will be run after each population is created, but before the population is passed to the objective function. This allows the user to impose integer/cardinality constriants.
`...`	further arguments to be passed to `fn`.

Details

`DEoptim` performs optimization (minimization) of `fn`.

The `control` argument is a list; see the help file for `DEoptim.control` for details.

The `R` implementation of Differential Evolution (DE), **DEoptim**, was first published on the Comprehensive `R` Archive Network (CRAN) in 2005 by David Ardia. Early versions were written in pure `R`. Since version 2.0-0 (published to CRAN in 2009) the package has relied on an interface to a C implementation of DE, which is significantly faster on most problems as compared to the implementation in pure `R`. The C interface is in many respects similar to the MS Visual C++ v5.0 implementation of the Differential Evolution algorithm distributed with the book *Differential Evolution – A Practical Approach to Global Optimization* by Price, K.V., Storn, R.M., Lampinen J.A, Springer-Verlag, 2006, and found on-line at http://www1.icsi.berkeley.edu/~storn/code.html. Since version 2.0-3 the C implementation dynamically allocates the memory required to store the population, removing limitations on the number of members in the population and length of the parameter vectors that may be optimized. Since version 2.2-0, the package allows for parallel operation, so that the evaluations of the objective function may be performed using all available cores. This is accomplished using either the built-in **parallel** package or the **foreach** package. If parallel operation is desired, the user should set `parallelType` and make sure that the arguments and packages needed by the objective function are available; see `DEoptim.control`, the example below and examples in the sandbox directory for details.

Figure 7. *DEoptim* documentation for RStudio

4 An Illustrative Example – City of London Gauging Station

The step-by-step procedure followed by the IDF_CC tool for updating IDF curves under nonstationary conditions is presented here.

1) To update the IDF curves use three datasets: (i) the sub-daily maximums from the observed data at a given location (i.e., maximums of 5min, 10min, 15min, 30min, 1hr, 2hr, 6hr, 12hr, 24hr precipitation data); (ii) daily maximums for the base period from the selected GCM model(s); and (iii) daily maximums from the RCP Scenarios (i.e., RCP 2.6, RCP 4.5, RCP 8.5) for the selected GCM model(s). All three datasets must be in chronological order. For this example, the series used are: 5-minute duration, GCM baseline (ensemble) and GCM (ensemble) future (RCP8.5) daily maximums. All three data sets are in Appendix B.
2) Fit the GEV probability distribution for each parameter combination from Table 1 to the 5-minute observed data series (1943-2016) using the Maximum Likelihood method. The obtained simulation results are as shown in Figure 8 and **Table 3**
3) Select the best model by using the corrected Akaike Information Criteria and then rank all the models. The GEV model with Δ_i equal to zero is classified as the best GEV model for the observed data by using the Equations 5 and 6. Table 4 presents the obtained results. Obtained results indicate the best GEV model is the stationary.

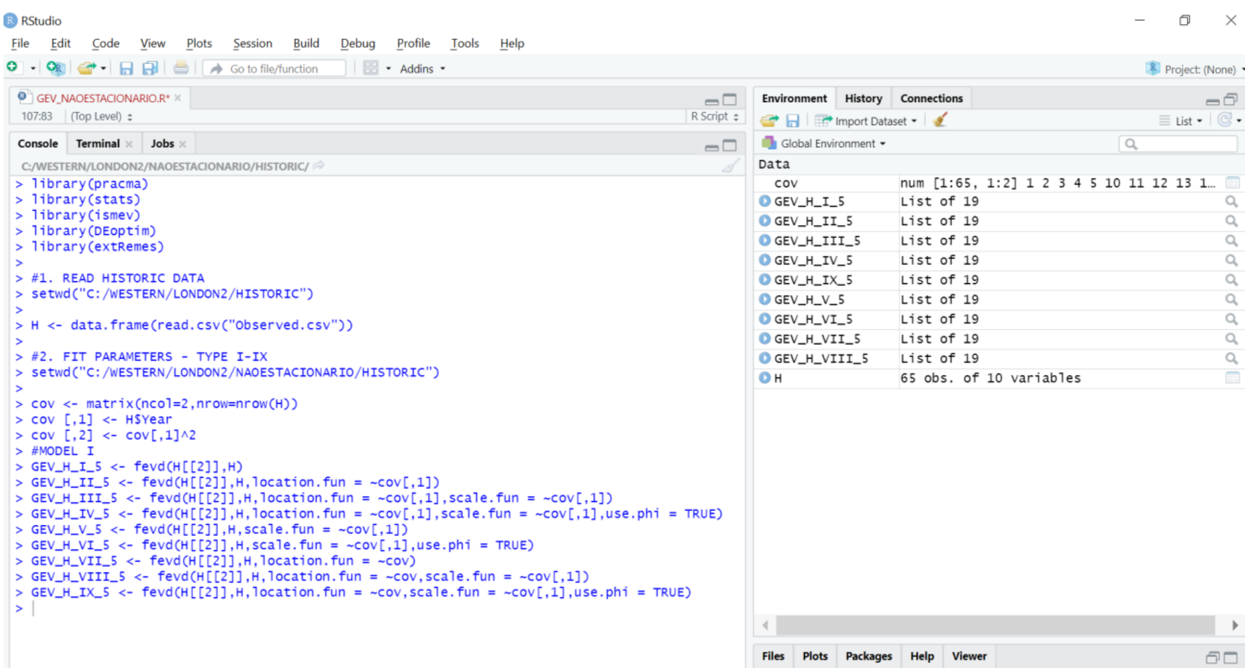

Figure 8. Simulation results obtained using RStudio (fitting observed data with 09 GEV model combinations)

Table 3. Fit parameters to 5-min precipitation data

Type of GEV model	Location	Shape	Scale	nllh
I	$\mu = 8.00$	$\sigma = 2.23$	$\xi = 0.063$	157.042
II	$\mu(t) = 8.17 - 0.00455t$	$\sigma = 2.22$	$\xi = 0.071$	156.979
III	$\mu(t) = 8.27 - 0.00674t$	$\sigma(t) = 2.39 - 0.00389t$	$\xi = 0.052$	156.916
IV	$\mu(t) = 8.28 - 0.00684t$	$\sigma(t) = \exp(0.88 - 0.00185t)$	$\xi = 0.051$	156.913
V	$\mu = 8.01$	$\sigma(t) = 2.30 - 0.00169t$	$\xi = 0.056$	157.028
VI	$\mu = 8.01$	$\sigma(t) = \exp(0.84 - 0.000803t)$	$\xi = 0.055$	157.027
VII	$\mu(t) = 8.06 + 0.00279t - 0.0000917t^2$	$\sigma = 2.22$	$\xi = 0.067$	156.970
VIII	$\mu(t) = 8.09 + 0.005834t - 0.000159t^2$	$\sigma(t) = 2.41 - 0.004433t$	$\xi = 0.053$	156.892
IX	$\mu(t) = 8.09 + 0.005907t - 0.000161t^2$	$\sigma(t) = \exp(0.88 - 0.0021t)$	$\xi = 0.052$	156.888

Table 4. Results obtained of AICc

Type of GEV model	k	AICc	Δ_i
I	3	320.478	0.00
II	4	322.642	2.16
III	5	324.850	4.37
IV	5	324.842	4.36
V	4	322.723	2.24
VI	4	322.722	2.24
VII	5	324.957	4.48
VIII	6	327.233	6.76
IX	6	327.225	6.75

4) In case of nonstationary GEV model being identified by AICc, test its significance using the Likelihood Test (Equation 7) by comparing it to the stationary model at $\chi^2(0.05)$ level of significance.
5) In case of significant nonstationary GEV model, extract the fit parameters by assuming the 95th percentiles for location and/or scale parameters, pending on the type of GEV model and its parameter equation.
6) Fit the GEV probability distribution to: (i) daily maximums from the GCM model (1950-2016), and (ii) daily maximums from the RCP Scenario 8.5 (2020-2100) (Table **5**). Figure 9 presents how data can be modelled using *gev.fit* function.

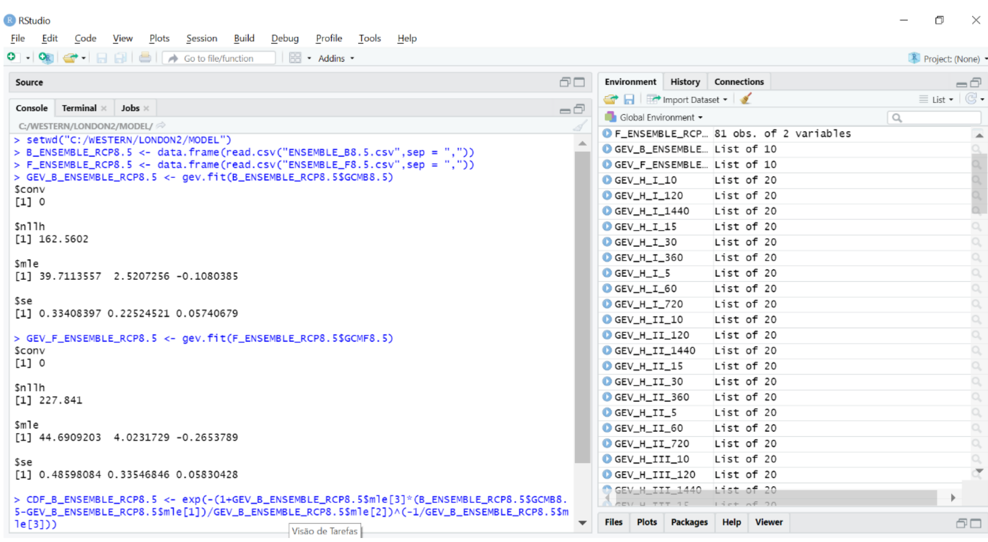

Figure 9. Fitting GEV distribution to GCM data

Table 5. GEV parameters for GCM data

	Location	**Shape**	**Scale**
GCM model baseline	39.711	2.52	-0.108
RCP 8.5	44.69	4.02	-0.266

7) Develop the relationship between the sub-daily observed maximums ($x_{j,o,h}$) and daily maximums obtained by GCM simulations for the baseline period (1950-2016) by finding the appropriate a_j, b_j, c_j and d_j coefficients of the Equation 7 (implementing the quantile matching to the inverse GEV distribution fitted to each series). The Figure 10 shows the example of Equation 7 development for sub-daily 5 minutes duration maximums and GCM baseline daily maximums. For this example, the coefficients of the fitted equation are: a_j = -18.797, b_j = 5.253, c_j = -0.0788 and d_j =-73.28 (Figure 11). Results indicate that OLS was well minimized, near zero value, as shown in Figure 11.

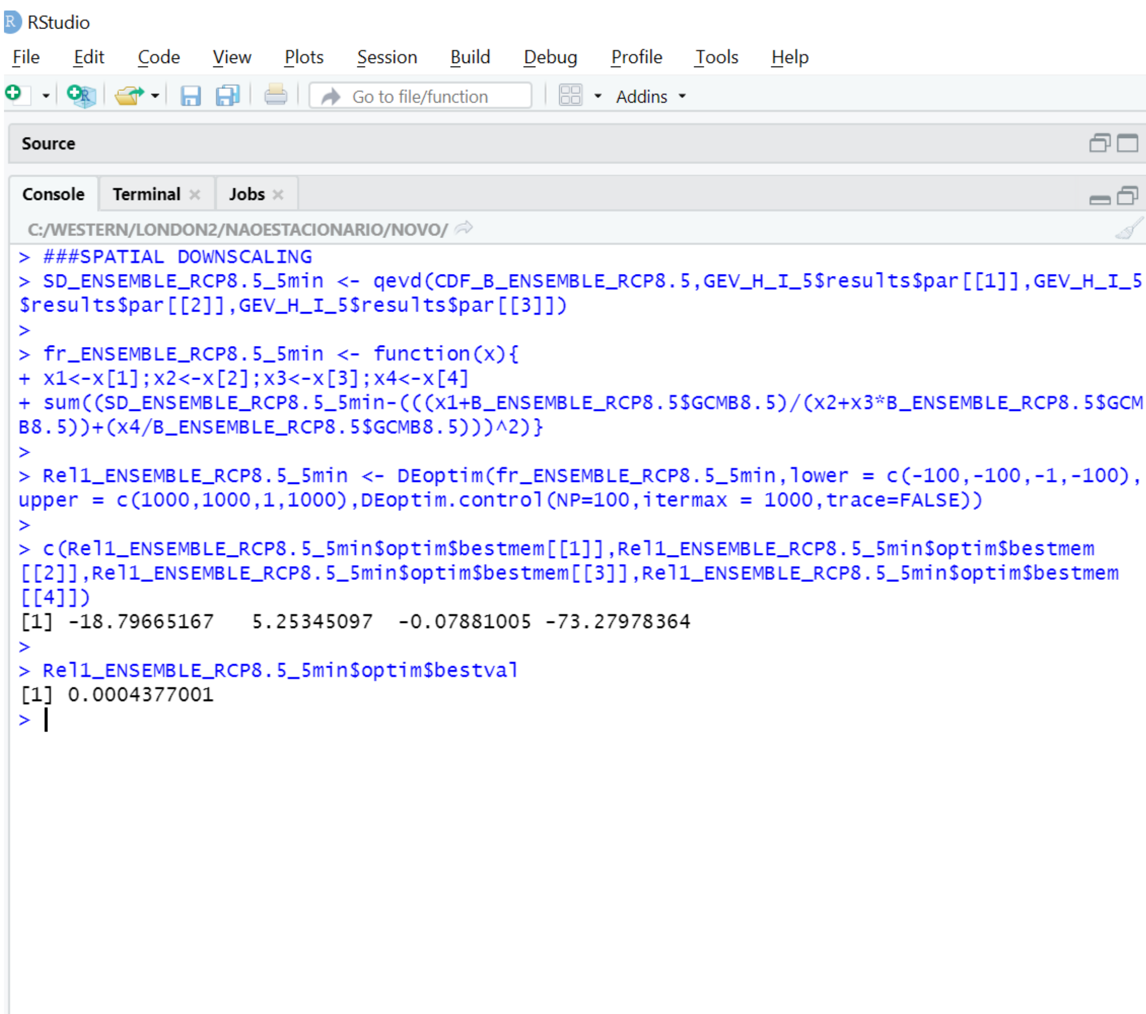

Figure 10. Simulated results for adjustment of coefficients of Equation 7

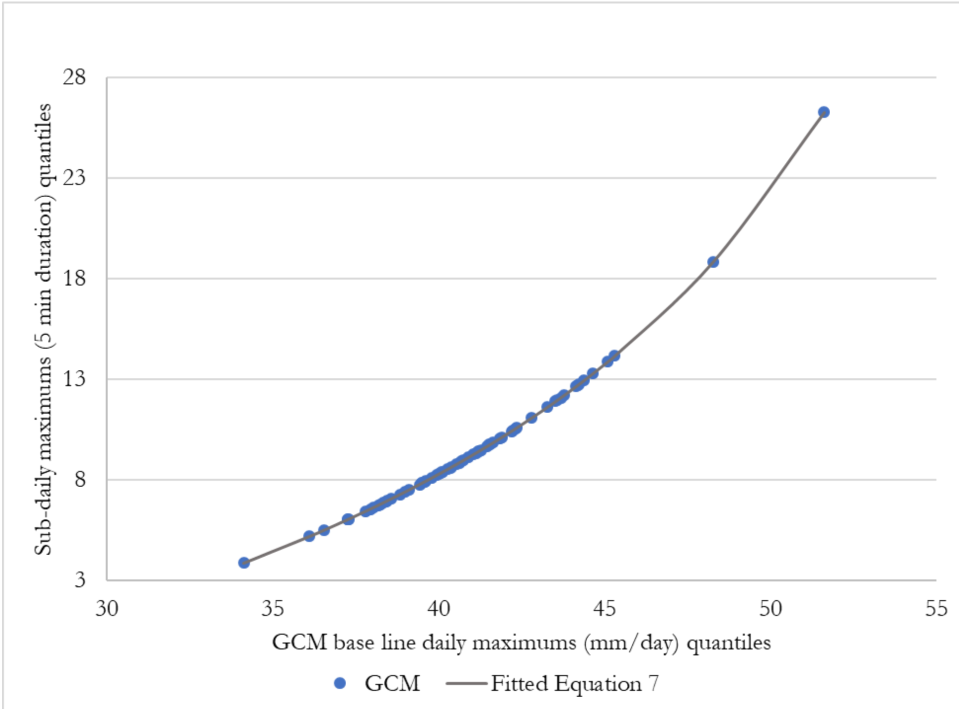

Figure 11. Quantile matching

8) Find the appropriate relative change Δ_m to relate $x_{m,h}$ and $x_{m,p}$ using Equations 8, 9 and 10. For the London station example, the future projected maximum for RCP 8.5, year 2020, with value of 44.38 mm/day is used (Appendix B), to calculate the corresponding 5-minute duration value at the station scale:

$$\tau_{m,f} = F_{m,f}\left(x_{m,f}\right) = F_{m,f}(44.380) = 0.33977$$
$$\hat{x}_{m,h} = F^{-1}{}_{m,h}\left(\tau_{m,f}\right) = F^{-1}{}_{m,h}(0.3397) = 39.5177$$
$$\Delta_m = \frac{44.38}{39.5177} = 1.123$$

9) From Equation 9 use $\hat{x}_{m,h}$ and fitted equation in Step 7 and multiply by the relative change Δ_m from Step 8 to obtain future projection data at London station.

$$\hat{x}_{j,o,h} = \frac{a_j + \hat{x}_{m,h}}{b_j + c_j\hat{x}_{m,h}} + \frac{d_j}{\hat{x}_{m,h}} = \frac{-18.797 + 39.5177}{5.253 + (-0.0788x39.5177)} + \frac{-73.28}{39.5177} = 7.833$$
$$x^f_{j,o,h} = \Delta_m . \hat{x}_{j,o,h} = 7.833x1.123 = 8.80$$

10) Repeat steps 2, 3, 4 and 5 to obtain the best GEV model and the fitted parameters for new future sub-daily data (95th percentiles if the best GEV model is non-stationary).
11) Obtain the return level estimation by applying the Equation 12 (Table 6).
12) The steps are repeated to all sub-daily durations and future RCPs to generate IDF curves for the future sub-daily data.

Table 6. Precipitation intensity results obtained for the London gauging station for 100year-return period

LONDON							
	Scenario				**Change in % from historical**		
Minutes	**Historical**	**RCP-2.6**	**RCP-4.5**	**RCP-8.5**	**RCP-2.6**	**RCP-4.5**	**RCP-8.5**
5	238.72	244.54	262.60	283.74	2.4%	10.0%	18.9%
10	221.01	219.75	273.15	287.92	-0.6%	23.6%	30.3%
15	170.84	171.07	204.31	221.75	0.1%	19.6%	29.8%
30	105.63	107.91	119.70	125.05	2.2%	13.3%	18.4%
60	70.43	71.16	83.47	92.28	1.0%	18.5%	31.0%
120	37.16	38.20	41.09	44.50	2.8%	10.6%	19.7%
360	13.82	14.06	15.51	16.24	1.8%	12.2%	17.5%
720	7.14	7.39	7.20	8.67	3.5%	0.9%	21.4%
1440	4.48	4.65	4.53	5.46	3.7%	1.0%	21.9%

5 Conclusions

In this report, we presented the methodology and its implementation for integrating the non-stationarity concept and climate change projections to estimate IDF curves for the future. First, the existence of trends in nine combinations of GEV parameters with time as covariate was investigated based on GEV distribution using method of maximum likelihood and tests to assess the statistical significance of the trend. The detection of trend(s) in GEV parameter(s) is used in IDFs generation, and a corresponding review of EQM method is proposed. The methodology is easy to implement and apply, being computationally efficient.

Unlike other methodologies to generate IDF curves under climate change, the methodology presented in this report is able to consider the non-stationary behavior of GEV distribution from the present to future time period. The EQM downscaling is revised and currently capable of considering both, the non-stationary and stationary GEV distributions.

We present an illustrative example using the London City gauging station. The main objective of the London City example is to present a detailed process of methodology implementation. In addition, the obtained results show that (a) different intensity precipitation increase for different durations; and (b) there is an increase in intensities in the future, except for 10 min duration for various RCP scenarios under non-stationary conditions and the time as covariate.

6 Acknowledgments

The authors thank the financial support from the "*Coordenação de Aperfeiçoamento de Pessoal de Nível Superior*" (CAPES-PRINT) – Grant numbers 88887.363277/2019-00, and Collaborative Research Grant provided by the Natural Sciences and Engineering Research Council of Canada and Chaucer Re.

References

Agilan, V., and N. V. Umamahesh, (2015) Detection and attribution of non-stationarity in intensity and frequency of daily and 4-hr extreme rainfall of Hyderabad, India, *Journal of Hydrology*, 530, 677-697. http://dx.doi.org/10.1016/j.jhydrol.2015.10.028.

Agilan, V., and N. V. Umamahesh, (2017) What are the best covariates for developing non-stationary rainfall Intensity-Duration-Frequency relationship, *Advances in Water Resources*, 101, 11-22. http://dx.doi.org/10.1016/j.advwatres.2016.12.2016.

Ardia, D., K. Mullen, B. Peterson, J. Ulrich, and K. Boudt (2020) Global Optimization by Differential Evolution. Version 2.2-5. Available for download on: https://cran.r-project.org/web/packages/DEoptim/DEoptim.pdf.

Cheng, L., A. AghaKouchak, E. Grilleland, and R. W. Katz, (2014). Non-stationary extreme value analysis in a changing climate, *Climatic Change*, 127, 353-369. DOI: 10.1007/s10584-014-1254-5.

Cheng, L., and A. AghaKouckak, (2014) Nonstationary Precipitation Intensity-Duration-Frequency Curves for Infrastructure Design in a Changing Climate, *Scientific Reports*, 4:7093. DOI: 10.1038/srep07093.

Coles, S., (2001) An Introduction To Statistical Modelling of Extreme Values. Springer, London.

CSA (Canadian Standards Association), (2012) Technical guide: Development, interpretation, and use of rainfall intensity-duration-frequency (IDF) information: Guideline for Canadian water resources practitioners. Mississauga: Canadian Standards Association.

Grilleland, E., (2019) Extreme Value Analysis. Version 2.0-10. Available for download on: http://www.ral.ucar.edu/staff/ericg/extRemes.

IPCC. (2014). Climate change 2014: Synthesis report. Contribution of Working Groups I, II and III to the Fifth Assessment Report of the Intergovernmental Panel on Climate Change [Pachauri, R. K.; and Meyer, L. A. (eds.)]. IPCC, Geneva, Switzerland, 151p.

Katz, R.W. et al., (2013) Statistical methods for nonstationary extremes. In: Kouchak, A. A., et al. (Eds.). Extremes in a Changing Climate: Detection, Analysis and Uncertainty. Springer, Dordrecht, pp. 15-37.

Millington, N., S. Das and S.P. Simonovic, (2011) The Comparison of GEV, Log-Pearson Type 3 and Gumbel Distributions in the Upper Thames River Watershed under Global Climate Models. *Water Resources Research Report no. 077*, Facility for Intelligent Decision Support, Department of Civil and Environmental Engineering, London, Ontario, Canada, 53 pages. ISBN: (print) 978-0-7714-2898-2; (online) 978-0-7714-2905-7.

Mondal, A., and P.P. Mujumdar, (2015) Modeling non-stationarity in intensity, duration and frequency of extreme rainfall over India, *Journal of Hydrology*, 521:217-231. DOI: 10.1006/j.jhydrol.2014.11.071.

Olsson, J., K. Berggren, M. Olofsson, and M. Viklander, (2009) Applying climate model precipitation scenarios for urban hydrological assessment: A case study in Kalmar City, Sweden. *Atmos. Res.*, 92:364–375, doi:10.1016/j.atmosres.2009.01.015.

Ouarda, T. B. J., L. A. Yousef, and C. Charron, (2018) Non-stationary intensity-duration-frequency curves integrating information concerning teleconnections and climate change, *International Journal of Climatology*, 2018, 1-8. DOI: 10.1002/joc.5953.

Overeem, A., A. Buishand, and I. Holleman, (2007) Rainfall depth-duration-frequency curves and their uncertainties, *Journal of Hydrology*, 348(1-2):124-134. DOI:10.1016/j.jhydrol.2007.09.044.

Peck, A., P. Prodanovic, and S.P. Simonovic, (2012) Rainfall Intensity Duration Frequency Curves Under Climate Change: City of London, Ontario, Canada. *Canadian Water Resources Journal*, 37(3):177–189.

R Development Core Team (2011) R: a language and environment for statistical computing. R Foundation for Statistical Computing, Vienna. http://www.R-project.org.

Schardong, A., S.P. Simonovic, A. Gaur and D. Sandink, (2020) Web-based Tool for the Development of Intensity Duration Frequency Curves under Changing Climate at Gauged and Ungauged Locations in Canada", under review, Water.

Simonovic, S.P., A. Schardong, D. Sandink, and R. Srivastav, (2016) A Web-based Tool for the Development of Intensity Duration Frequency Curves under Changing Climate, E*nvironmental Modelling & Software Journal,* 81:136-153.

Solaiman, T.A., and S.P. Simonovic, (2010) National centers for environmental prediction -national center for atmospheric research (NCEP-NCAR) reanalyses data for hydrologic modelling on a basin scale (2010) *Canadian Journal of Civil Engineering*, 37(4):611-623.

Srivastav, R.K., A. Schardong, and S. P. Simonovic, (2014) Equidistance Quantile Matching Method for Updating IDF Curves under Climate Change, *Water Resources Management*, 28(9): 2539-2562.

Sugahara, S., R.P. Rocha, and R. Silveira, (2009) Non-stationary frequency analysis of extreme daily rainfall in Sao Paulo, Brazil, 29, 1339–1349. doi:10.1002/joc.

Appendix A: GCMs used

The selected biased corrected downscaled CMIP5 climate models and their attributes which has all three emissions scenarios (RCP2.6, RCP4.5 and RCP8.5) used in the presented study.

Bias Correction	Model	Country	Centre Name
BCCAQv2	bcc-csm1-1	China	Beijing Climate Center, China Meteorological Administration
BCCAQv2	bcc-csm1-1-m	China	Beijing Climate Center, China Meteorological Administration
BCCAQv2	BNU-ESM	China	College of Global Change and Earth System Science
BCCAQv2	CanESM2	Canada	Canadian Centre for Climate Modeling and Analysis
BCCAQv2	CCSM4	USA	National Center of Atmospheric Research
BCCAQv2	CESM1-CAM5	USA	National Center of Atmospheric Research
BCCAQv2	CNRM-CM5	France	Centre National de Recherches Meteorologiques and Centre Europeen de Recherches et de Formation Avancee en Calcul Scientifique
BCCAQv2	CSIRO-Mk3-6-0	Australia	Australian Commonwealth Scientific and Industrial Research Organization in collaboration with the Queensland Climate Change Centre of Excellence
BCCAQv2	FGOALS-g2	China	IAP (Institute of Atmospheric Physics, Chinese Academy of Sciences, Beijing, China) and THU (Tsinghua University)
BCCAQv2	GFDL-CM3	USA	National Oceanic and Atmospheric Administration's Geophysical Fluid Dynamic Laboratory
BCCAQv2	GFDL-ESM2G	USA	National Oceanic and Atmospheric Administration's Geophysical Fluid Dynamic Laboratory
BCCAQv2	HadGEM2-AO	United Kingdom	Met Office Hadley Centre
BCCAQv2	HadGEM2-ES	United Kingdom	Met Office Hadley Centre
BCCAQv2	IPSL-CM5A-LR	France	Institut Pierre Simon Laplace
BCCAQv2	IPSL-CM5A-MR	France	Institut Pierre Simon Laplace
BCCAQv2	MIROC5	Japan	Japan Agency for Marine-Earth Science and Technology
BCCAQv2	MIROC-ESM	Japan	Japan Agency for Marine-Earth Science and Technology
BCCAQv2	MIROC-ESM-CHEM	Japan	Japan Agency for Marine-Earth Science and Technology
BCCAQv2	MPI-ESM-LR	Germany	Max Planck Institute for Meteorology
BCCAQv2	MPI-ESM-MR	Germany	Max Planck Institute for Meteorology

BCCAQv2	MRI-CGCM3	Japan	Meteorological Research Institute
BCCAQv2	NorESM1-M	Norway	Norwegian Climate Center
BCCAQv2	NorESM1-ME	Norway	Norwegian Climate Center
BCCAQv2	GFDL-ESM2M	USA	National Oceanic and Atmospheric Administration's Geophysical Fluid Dynamic Laboratory

Appendix B: Case Study Example: London Station, Ontario

The following is the observed annual maximum precipitation for London gauging station obtained from Environment and Climate Change Canada for the duration of 5min, 10min, 15min, 30min, 1hr, 2hr, 6hr, 12hr and 24hr.

Year	**DURATION (min)**								
	5	**10**	**15**	**30**	**60**	**120**	**360**	**720**	**1440**
1943	18.3	24.1	26.2	36.3	51.1	53.8	53.8	56.1	78.7
1944	7.6	8.1	11.2	15.2	21.1	34.3	47.0	51.8	56.1
1945	6.6	9.7	12.7	17.3	19.3	25.4	34.3	39.4	47.8
1946	13.2	14.5	15.5	29.7	48.3	60.5	61.5	61.5	83.3
1947	10.9	19.3	23.9	29.2	29.2	29.2	40.9	43.2	46.7
1952	7.9	12.7	15.2	28.7	30.5	30.5	38.4	39.9	74.2
1953	15.7	24.6	36.8	56.9	83.3	83.3	83.3	83.3	83.3
1954	10.9	12.7	17.0	21.6	29.2	32.8	39.1	52.6	78.0
1955	6.6	9.1	11.2	14.2	14.7	17.3	32.5	44.2	51.1
1956	9.1	10.7	11.7	16.8	20.1	35.3	40.4	42.7	53.8
1957	6.3	9.4	12.4	16.5	26.2	28.2	35.6	47.5	55.6
1958	7.6	9.7	11.2	15.7	16.5	18.5	29.2	39.1	39.9
1959	8.6	10.9	13.0	15.5	23.4	39.6	50.3	50.5	50.5
1960	9.1	12.7	16.8	27.7	28.2	38.9	39.9	42.4	46.7
1961	11.4	20.1	23.9	29.0	39.9	43.2	43.4	43.4	43.4
1962	8.6	16.5	17.0	17.0	18.8	26.7	29.0	34.8	35.1
1963	5.6	7.9	9.1	10.4	10.4	11.4	21.3	21.3	23.9
1964	7.9	10.9	14.2	19.0	23.9	32.3	38.1	59.2	67.3
1965	5.6	10.4	11.7	14.2	18.3	21.1	29.0	38.4	43.7
1966	8.4	8.4	8.9	14.2	19.3	27.4	43.9	52.6	52.6
1967	7.9	11.9	12.2	19.3	20.6	22.4	33.5	37.3	41.4

1968	10.4	13.2	16.0	24.6	28.7	32.3	53.1	67.6	84.6
1969	6.9	10.2	13.5	15.7	15.7	18.5	27.4	39.9	47.5
1970	10.9	13.0	16.5	17.0	21.1	22.1	23.9	33.3	36.8
1971	8.9	15.0	22.4	32.5	39.1	42.7	42.7	42.7	42.7
1972	14.5	20.1	22.9	22.9	34.3	40.6	58.4	59.7	62.5
1973	7.4	9.4	13.5	17.0	17.8	19.6	31.5	40.4	52.1
1974	4.8	7.9	9.1	10.9	13.2	22.4	29.2	30.2	35.3
1975	9.1	12.4	15.2	18.5	21.1	21.1	27.9	30.5	30.5
1976	18.5	26.9	27.7	29.2	30.5	30.7	37.8	40.9	50.0
1978	6.6	10.9	14.2	14.4	14.4	14.4	23.5	27.3	29.6
1979	19.2	33.5	37.6	45.9	46.0	46.0	46.6	65.4	68.2
1980	11.5	20.6	27.8	30.6	32.5	32.6	37.7	47.1	61.7
1981	10.1	12.5	13.2	13.2	16.2	26.7	35.0	37.5	43.5
1982	6.8	10.8	15.1	22.2	24.6	28.6	35.4	36.8	37.6
1983	13.5	23.4	29.5	37.6	41.1	41.1	47.0	55.8	64.4
1984	9.8	10.6	14.5	27.4	27.8	43.5	50.8	56.0	69.7
1985	8.3	10.9	13.7	22.8	29.0	35.1	43.2	56.8	65.0
1986	12.4	22.7	24.2	24.5	30.6	42.2	43.8	49.7	89.1
1987	6.7	9.4	11.0	13.2	14.3	17.7	27.2	44.5	56.5
1988	7.9	11.2	15.5	18.2	18.3	26.9	33.0	41.9	61.6
1989	8.7	10.9	13.5	23.3	25.7	25.8	25.8	34.0	34.8
1990	11.9	16.7	18.7	30.4	35.1	37.9	41.6	54.1	75.5
1991	9.7	11.6	13.9	17.5	20.6	22.0	28.1	32.2	32.2
1992	6.5	11.5	15.9	20.9	35.0	45.2	51.8	58.6	76.3
1993	9.4	14.3	15.1	19.1	21.9	25.0	28.5	30.7	49.2
1994	7.5	11.3	12.1	16.8	20.6	33.2	38.9	40.3	46.5
1995	8.2	11.3	12.6	15.8	21.8	28.0	37.8	45.0	56.1

1996	9.4	15.8	17.9	26.1	39.2	68.1	82.7	83.5	89.0
1997	10.6	17.0	19.6	21.8	21.8	24.8	31.1	33.9	33.9
1998	12.6	14.7	15.8	17.6	20.4	20.4	20.4	-99.9	33.0
1999	7.3	11.2	11.8	12.7	13.3	19.0	25.9	26.1	32.9
2000	11.5	15.3	17.6	23.0	30.6	40.6	-99.9	-99.9	82.8
2001	6.3	7.9	10.6	13.2	13.4	14.0	24.0	35.0	41.2
2003	10.0	18.4	32.2	26.2	26.2	27.8	31.2	40.8	40.8
2004	15.0	23.6	27.2	29.4	29.4	29.6	45.4	47.0	47.0
2005	9.0	12.6	15.4	19.8	19.8	24.0	35.6	37.0	45.6
2006	12.6	22.0	26.6	28.0	42.4	46.4	49.0	49.0	77.2
2007	7.0	12.4	14.6	14.6	17.2	22.4	30.4	30.6	30.6
2009	7.8	11.4	12.0	17.0	17.0	19.8	29.4	35.0	43.0
2010	10.0	14.4	20.4	29.4	32.6	33.0	33.8	34.2	42.4
2011	6.8	11.6	17.2	29.2	35.8	35.8	40.6	44.0	44.0
2012	4.4	6.8	8.4	9.2	12.4	16.8	25.6	30.6	32.4
2013	8.0	11.2	15.0	20.0	24.2	30.8	51.8	80.0	96.0
2014	9.6	16.6	23.6	31.6	41.6	50.0	59.8	62.2	63.2
2015	8.8	14.2	19.6	23.8	23.8	34.0	34.8	42.6	42.6
2016	11.0	19.0	21.4	35.6	38.4	42.4	44.8	58.8	68.8

The ensemble GCM data for the base period at London gauging station:

Year	**PPT (mm/day)** **GCM ensemble Base period**
1950	38.515
1951	40.450
1952	41.275
1953	39.865

1954	34.140
1955	39.190
1956	39.155
1957	40.125
1958	40.620
1959	41.470
1960	42.860
1961	40.555
1962	39.125
1963	35.935
1964	38.980
1965	44.390
1966	37.190
1967	37.130
1968	41.780
1969	41.860
1970	41.195
1971	39.695
1972	40.135
1973	43.550
1974	37.460
1975	42.265
1976	39.670
1977	39.570
1978	40.015
1979	40.315
1980	41.510

1981	40.055
1982	40.035
1983	46.045
1984	38.040
1985	41.850
1986	37.630
1987	43.710
1988	39.540
1989	40.840
1990	45.065
1991	45.750
1992	38.380
1993	39.385
1994	41.265
1995	37.910
1996	39.955
1997	41.845
1998	43.545
1999	42.140
2000	48.680
2001	42.165
2002	42.245
2003	44.650
2004	50.590
2005	40.000
2006	39.960
2007	43.485

2008	44.610
2009	49.915
2010	42.180
2011	43.955
2012	39.540
2013	37.815
2014	40.460
2015	41.625
2016	47.980

The future GCM ensemble data for London gauging station:

Year	**PPT (mm/day) – GCM ensemble future**		
	RCP 2.6	**RCP 4.5**	**RCP 8.5**
2020	43.350	40.450	44.380
2021	38.690	40.825	44.230
2022	37.085	40.155	38.915
2023	41.280	40.875	36.275
2024	40.930	44.005	48.525
2025	40.505	41.995	53.110
2026	38.650	38.375	43.375
2027	46.125	43.190	40.700
2028	41.580	38.915	42.070
2029	45.300	39.790	45.845
2030	42.300	42.965	42.935
2031	42.995	41.805	43.220
2032	40.455	40.500	45.890
2033	43.890	41.205	37.885
2034	44.060	44.175	42.505

2035	44.260	41.085	41.730
2036	40.015	43.995	37.175
2037	47.675	47.390	45.190
2038	41.815	38.905	44.435
2039	37.990	44.025	44.215
2040	44.630	46.165	39.610
2041	47.090	46.465	44.845
2042	42.040	43.265	45.80
2043	41.810	42.330	48.865
2044	44.565	43.850	43.345
2045	43.945	44.130	39.940
2046	48.080	46.640	45.080
2047	47.160	47.965	45.560
2048	43.715	39.915	41.775
2049	40.770	42.120	44.22
2050	51.205	38.57	46.515
2051	40.620	44.960	45.660
2052	43.145	41.920	46.705
2053	44.295	47.545	49.270
2054	42.370	46.005	40.265
2055	41.750	44.700	44.385
2056	43.630	49.505	41.420
2057	42.265	43.255	49.650
2058	41.660	42.680	46.130
2059	46.895	47.080	46.635
2060	51.965	41.615	45.980
2061	40.555	45.620	43.640

2062	43.980	45.715	45.160
2063	45.615	47.205	45.095
2064	43.780	43.110	43.530
2065	44.540	48.035	44.970
2066	41.390	48.415	51.64
2067	43.645	46.460	47.480
2068	43.875	42.455	46.330
2069	45.260	42.840	52.505
2070	45.670	45.780	42.220
2071	41.750	47.110	47.400
2072	44.165	42.590	44.120
2073	44.360	44.810	48.030
2074	45.905	41.905	47.865
2075	45.975	41.475	42.430
2076	39.345	44.190	50.950
2077	44.925	45.370	45.795
2078	41.640	47.715	52.285
2079	43.105	44.805	49.715
2080	41.685	44.680	56.890
2081	43.025	38.795	48.965
2082	42.850	45.915	45.980
2083	37.840	43.455	49.210
2084	43.910	41.615	49.530
2085	44.325	45.405	47.265
2086	46.885	49.915	47.710
2087	45.470	48.225	51.540
2088	45.415	44.3900	52.040

2089	46.345	45.540	52.070
2090	44.435	44.710	46.960
2091	41.035	44.090	49.530
2092	36.335	42.800	53.720
2093	43.725	44.045	44.915
2094	45.950	45.840	45.090
2095	40.805	40.745	52.230
2096	40.605	44.700	49.505
2097	46.365	41.390	52.010
2098	39.920	42.900	47.895
2099	41.570	44.400	48.665
2100	39.690	37.650	50.680

Appendix c: RStudio Code for Updating Idf Curves (London City Example)

UPDATE IDF CURVES – Rstudio CODE

Contents

- Intensity-Duration-Frequency Curves Under Climate Change
- Clear Workspace and Command Window
- Input Data
- FIT Extreme value distribution
- Install packages

Packages to be install: ismev, extRemes, and DEoptim

#Author: Daniele F. Silva

#Method: Equidistant Quantile Matching under Non-Stationarity

- **Open the packages**

```
library(ismev)
library(DEoptim)
library(extRemes)
```

#GENERATE GEV PARAMETERS for HISTORIC DATA

#Data is provided in .csv file

- **Read Historic Data**

```
setwd("directory where data is placed")
```

#Each Duration is treated independently since there is missing data for some rainfall durations

#Each rainfall duration data comprehends 2 columns, first with the chronological period (1,2,3,…,n), and second with the correspondent maximum precipitation. YearX is the the time (year) and H_Xmin is the correspondent precipitation. X remains to each duration.

#Read Historic Data

```
H <- data.frame(read.csv("Observed.csv"))
```

- **Fit parameters data – From type I to IX**

#Fit parameters – type I to IX

```
cov <- matrix(ncol=2,nrow=nrow(H))
cov[,1] <- H$Year
cov[,2] <- cov[,1]^2
```

#Model I

```
GEV_H_I_5 <- fevd(H[[2]],H)
```

#Model II

```
GEV_H_II_5 <- fevd(H[[2]],H,location.fun = ~ cov[,1])
```

#Model III

```
GEV_H_III_5 <- fevd(H[[2]],H,location.fun = ~ cov[,1],scale.fun = ~cov[,1])
```

#Model IV

```
GEV_H_IV_5 <- fevd(H[[2]],H,location.fun = ~ cov[,1],scale.fun = ~ cov[,1],use.phi = TRUE)
```

#Model V

```
GEV_H_V_5 <- fevd(H[[2]],H,scale.fun = ~ cov[,1])
```

#Model VI

```
GEV_H_VI_5 <- fevd(H[[2]],H, scale.fun = ~ cov[,1],use.phi = TRUE)
```

#Model VII

```
GEV_H_VII_5 <- fevd(H[[2]],H,location.fun = ~cov)
```

#Model VIII

```
GEV_H_VIII_5 <- fevd(H[[2]],H,location.fun = ~cov,scale.fun = ~ cov[,1])
```

#Model IX

```
GEV_H_IX_5 <- fevd(H[[2]],H,location.fun = ~cov,scale.fun = ~cov[,1],use.phi = TRUE)
```

- **Identification of the best model – AICc and ranked delta**

#AICc

```
AICc_H_5min <-
c(2*GEV_H_I_5$results$value+2*length(GEV_H_I_5$results$par)+2*length(GEV_H_I_5$results$par)*(length(GEV_H_I_5$results$par)+1)/(length(H[[2]])-length(GEV_H_I_5$results$par)-1),
2*GEV_H_II_5$results$value+2*length(GEV_H_II_5$results$par)+2*length(GEV_H_II_5$results$par)*(length(GEV_H_II_5$results$par)+1)/(length(H[[2]])-length(GEV_H_II_5$results$par)-1),
2*GEV_H_III_5$results$value+2*length(GEV_H_III_5$results$par)+2*length(GEV_H_III_5$results$par)*(length(GEV_H_III_5$results$par)+1)/(length(H[[2]])-length(GEV_H_III_5$results$par)-1),
2*GEV_H_IV_5$results$value+2*length(GEV_H_IV_5$results$par)+2*length(GEV_H_IV_5$results$par)*(length(GEV_H_IV_5$results$par)+1)/(length(H[[2]])-length(GEV_H_IV_5$results$par)-1),
2*GEV_H_V_5$results$value+2*length(GEV_H_V_5$results$par)+2*length(GEV_H_V_5$results$par)*(length(GEV_H_V_5$results$par)+1)/(length(H[[2]])-length(GEV_H_V_5$results$par)-1),
2*GEV_H_VI_5$results$value+2*length(GEV_H_VI_5$results$par)+2*length(GEV_H_VI_5$results$par)*(length(GEV_H_VI_5$results$par)+1)/(length(H[[2]])-length(GEV_H_VI_5$results$par)-1),
2*GEV_H_VII_5$results$value+2*length(GEV_H_VII_5$results$par)+2*length(GEV_H_VII_5$results$par)*(length(GEV_H_VII_5$results$par)+1)/(length(H[[2]])-length(GEV_H_VII_5$results$par)-1),
2*GEV_H_VIII_5$results$value+2*length(GEV_H_VIII_5$results$par)+2*length(GEV_H_VIII_5$results$par)*(length(GEV_H_VIII_5$results$par)+1)/(length(H[[2]])-length(GEV_H_VIII_5$results$par)-1),
2*GEV_H_IX_5$results$value+2*length(GEV_H_IX_5$results$par)+2*length(GEV_H_IX_5$results$par)*(length(GEV_H_IX_5$results$par)+1)/(length(H[[2]])-length(GEV_H_IX_5$results$par)-1))
```

#Delta

```
Delta_H_5min <- AICc_H_5min – min(AICc_H_5min)
```

- **Likelihood ratio test – Significance of the trend parameter**

```
LR_H_5min <- c(lr.test(GEV_H_I_5,GEV_H_I_5)$p.value,lr.test(GEV_H_I_5,GEV_H_II_5)$p.value,lr.test(GEV_H_I_5,GEV_H_III_5)$p.value,
lr.test(GEV_H_I_5,GEV_H_IV_5)$p.value,lr.test(GEV_H_I_5,GEV_H_V_5)$p.value,lr.test(GEV_H_I_5,GEV_H_VI_5)$p.value,
lr.test(GEV_H_I_5,GEV_H_VII_5)$p.value,lr.test(GEV_H_I_5,GEV_H_VIII_5)$p.value,lr.test(GEV_H_I_5,GEV_H_IX_5)$p.value)
```

#now it is necessary: (i) the best model, and (ii) if the best model is also significant. If some non-stationary model is selected as the best, calculate the parameters of distribution considering the 95th percentile.

#In this case, 5min duration series does not present non-stationary behavior.

- **Read GCM data**

#Read GCM data – baseline and future projection

```
B_MODEL_RCP8.5 <- data.frame(read.csv("MODEL_B8.5.csv",sep = ","))
F_MODEL_RCP8.5 <- data.frame(read.csv("MODEL_F8.5csv",sep = ","))
```

- **Fit Parameter Distribution and Calculate CDF for GCM data**

```
GEV_B_MODEL_RCP8.5 <- fevd(B_MODEL_RCP8.5$GCMB8.5,B_MODEL_RCP8.5)
```

```
GEV_F_MODEL_RCP8.5 <- fevd(F_MODEL_RCP8.5$GCMF8.5,F_MODEL_RCP8.5)
CDF_B_MODEL_RCP8.5 <- exp(-(1+GEV_B_ENSEMBLE_RCP8.5$results$par[3]*(B_ENSEMBLE_RCP8.5$GCMB8.5-GEV_B_ENSEMBLE_RCP8.5$ results$par [1])/GEV_B_ENSEMBLE_RCP8.5$ results$par [2])^(-1/GEV_B_ENSEMBLE_RCP8.5$ results$par [3]))
CDF_F_MODEL_RCP8.5 <- exp(-(1+GEV_F_ENSEMBLE_RCP8.5$results$par[3]*(F_ENSEMBLE_RCP8.5$GCMF8.5-GEV_F_ENSEMBLE_RCP8.5$ results$par [1])/GEV_F_ENSEMBLE_RCP8.5$ results$par [2])^(-1/GEV_F_ENSEMBLE_RCP8.5$ results$par [3]))
```

- **Downscaling**

```
#Spatial Downscaling – relationship between historic data and GCM baseline data

SD_MODEL_RCP8.5_5min<-
qevd(CDF_B_MODEL_RCP8.5,GEV_H_I_5$results$par[[1]],GEV_H_I_5$results$par[[2]],GEV_H_I_5$results$par[[3]])

#Find the adjusted parameters

fr_MODEL_RCP2.6_5min <- function(x){
  x1<-x[1];x2<-x[2];x3<-x[3];x4<-x[4]
  sum((SD_MODEL_RCP8.5_5min-
(((x1+B_MODEL_RCP8.5$GCMB8.5)/(x2+x3*B_MODEL_RCP8.5$GCMB8.5))+(x4/B_MODEL_RCP8.5$GCMB8.5)))^2)}

Rel1_MODEL_RCP8.5_5min <- DEoptim(fr_ENSEMBLE_RCP8.5_5min,lower = c(-100,-1000,-1,-100),upper = c(1000,1000,1,1000),DEoptim.control(NP=100,itermax = 1000,trace=FALSE))
#Temporal Downscaling – relationship between GCM baseline and future periods.
TD_MODEL_RCP8.5 <-
qevd(CDF_F_MODEL_RCP8.5,GEV_B_MODEL_RCP8.5$results$par[[1]],GEV_B_MODEL_RCP8.5$results$par[[2]],GEV_B_MODEL_RCP8.5$results$par[[3]])
#Scaling Factor
Rel2_MODEL_RCP8.5 <- F_MODEL_RCP8.5$GCMF8.5/TD_MODEL_RCP8.5
```

- **Future Sub-daily data**

```
#Future sub-daily data

NEW_MODEL_RCP8.5_5 <-
(((Rel1_MODEL_RCP8.5_5min$optim$bestmem[[1]]+TD_MODEL_RCP8.5)/(Rel1_MODEL_RCP8.5_5min$optim$bestmem[[2]]+(Rel1_MODEL_RCP8.5_5min$optim$bestmem[[3]]*TD_MODEL_RCP8.5)))+((Rel1_MODEL_RCP8.5_5min$optim$bestmem[[4]]/TD_MODEL_RCP8.5)))*Rel2_MODEL_RCP8.5
```

- **Identify Non-Stationarity in future sub-daily data**

```
#Fit parameters distributions for all nine GEV models, identify the best one and tests its significance against the stationary model.

ti_MODEL_RCP8.5 <- matrix(ncol=2,nrow=nrow(NEW_MODEL_RCP8.5))
ti_MODEL_RCP8.5[,1] <- Year_MODEL_RCP8.5
ti_MODEL_RCP8.5[,2] <- ti_MODEL_RCP8.5[,1]^2
GEV_NEW_MODEL_RCP8.5_I_5 <- fevd(NEW_MODEL_RCP8.5[[1]],NEW_MODEL_RCP8.5)
GEV_NEW_MODEL_RCP8.5_II_5 <- fevd(NEW_MODEL_RCP8.5[[1]],NEW_MODEL_RCP8.5,location.fun = ~Year_MODEL_RCP8.5)
GEV_NEW_MODEL_RCP8.5_III_5 <- fevd(NEW_MODEL_RCP8.5[[1]],NEW_MODEL_RCP8.5,location.fun = ~Year_MODEL_RCP8.5,scale.fun = ~Year_MODEL_RCP8.5)
GEV_NEW_MODEL_RCP8.5_IV_5 <- fevd(NEW_MODEL_RCP8.5[[1]],NEW_MODEL_RCP8.5,location.fun = ~Year_MODEL_RCP8.5,scale.fun = ~Year_MODEL_RCP8.5,use.phi = TRUE)
GEV_NEW_MODEL_RCP8.5_V_5 <- fevd(NEW_MODEL_RCP8.5[[1]],NEW_MODEL_RCP8.5,scale.fun = ~Year_MODEL_RCP8.5)
GEV_NEW_MODEL_RCP8.5_VI_5 <- fevd(NEW_MODEL_RCP8.5[[1]],NEW_MODEL_RCP8.5,scale.fun = ~Year_MODEL_RCP8.5,use.phi = TRUE)
GEV_NEW_MODEL_RCP8.5_VII_5 <- fevd(NEW_MODEL_RCP8.5[[1]],NEW_MODEL_RCP8.5,location.fun = ~ti_MODEL_RCP8.5)
GEV_NEW_MODEL_RCP8.5_VIII_5 <- fevd(NEW_MODEL_RCP8.5[[1]],NEW_MODEL_RCP8.5,location.fun = ~ti_MODEL_RCP8.5,scale.fun = ~Year_MODEL_RCP8.5)
GEV_NEW_MODEL_RCP8.5_IX_5 <- fevd(NEW_MODEL_RCP8.5[1]],NEW_MODEL_RCP8.5,location.fun = ~ti_MODEL_RCP8.5,scale.fun = ~Year_MODEL_RCP8.5,use.phi = TRUE)



#AICc – new sub-daily data

AICc_NEW_MODEL_RCP8.5_5 <-
c(2*GEV_NEW_MODEL_RCP8.5_I_5$results$value+2*length(GEV_NEW_MODEL_RCP8.5_I_5$results$par)+2*length(GEV_NEW_MODEL
```

```
_RCP8.5_I_5$results$par)*(length(GEV_NEW_MODEL_RCP8.5_I_5$results$par)+1)/(length(NEW_MODEL_RCP8.5[[1]])-length(GEV_NEW_MODEL_RCP8.5_I_5$results$par)-1),2*GEV_NEW_MODEL_RCP8.5_II_5$results$value+2*length(GEV_NEW_MODEL_RCP8.5_II_5$results$par)+2*length(GEV_NEW_MODEL_RCP8.5_II_5$results$par)*(length(GEV_NEW_MODEL_RCP8.5_II_5$results$par)+1)/(length(NEW_MODEL_RCP8.5[[1]])-length(GEV_NEW_MODEL_RCP8.5_II_5$results$par)-1),2*GEV_NEW_MODEL_RCP8.5_III_5$results$value+2*length(GEV_NEW_MODEL_RCP8.5_III_5$results$par)+2*length(GEV_NEW_MODEL_RCP8.5_III_5$results$par)*(length(GEV_NEW_MODEL_RCP8.5_III_5$results$par)+1)/(length(NEW_MODEL_RCP8.5[[1]])-length(GEV_NEW_MODEL_RCP8.5_III_5$results$par)-1),2*GEV_NEW_MODEL_RCP8.5_IV_5$results$value+2*length(GEV_NEW_MODEL_RCP8.5_IV_5$results$par)+2*length(GEV_NEW_MODEL_RCP8.5_IV_5$results$par)*(length(GEV_NEW_MODEL_RCP8.5_IV_5$results$par)+1)/(length(NEW_MODEL_RCP8.5[[1]])-length(GEV_NEW_MODEL_RCP8.5_IV_5$results$par)-1),2*GEV_NEW_MODEL_RCP8.5_V_5$results$value+2*length(GEV_NEW_MODEL_RCP8.5_V_5$results$par)+2*length(GEV_NEW_MODEL_RCP8.5_V_5$results$par)*(length(GEV_NEW_MODEL_RCP8.5_V_5$results$par)+1)/(length(NEW_MODEL_RCP8.5[[1]])-length(GEV_NEW_MODEL_RCP8.5_V_5$results$par)-1),2*GEV_NEW_MODEL_RCP8.5_VI_5$results$value+2*length(GEV_NEW_MODEL_RCP8.5_VI_5$results$par)+2*length(GEV_NEW_MODEL_RCP8.5_VI_5$results$par)*(length(GEV_NEW_MODEL_RCP8.5_VI_5$results$par)+1)/(length(NEW_MODEL_RCP8.5[[1]])-length(GEV_NEW_MODEL_RCP8.5_VI_5$results$par)-1),2*GEV_NEW_MODEL_RCP8.5_VII_5$results$value+2*length(GEV_NEW_MODEL_RCP8.5_VII_5$results$par)+2*length(GEV_NEW_MODEL_RCP8.5_VII_5$results$par)*(length(GEV_NEW_MODEL_RCP8.5_VII_5$results$par)+1)/(length(NEW_MODEL_RCP8.5[[1]])-length(GEV_NEW_MODEL_RCP8.5_VII_5$results$par)-1),2*GEV_NEW_MODEL_RCP8.5_VIII_5$results$value+2*length(GEV_NEW_MODEL_RCP8.5_VIII_5$results$par)+2*length(GEV_NEW_MODEL_RCP8.5_VIII_5$results$par)*(length(GEV_NEW_MODEL_RCP8.5_VIII_5$results$par)+1)/(length(NEW_MODEL_RCP8.5[[1]])-length(GEV_NEW_MODEL_RCP8.5_VIII_5$results$par)-1),2*GEV_NEW_MODEL_RCP8.5_IX_5$results$value+2*length(GEV_NEW_MODEL_RCP8.5_IX_5$results$par)+2*length(GEV_NEW_MODEL_RCP8.5_IX_5$results$par)*(length(GEV_NEW_MODEL_RCP8.5_IX_5$results$par)+1)/(length(NEW_MODEL_RCP8.5[[1]])-length(GEV_NEW_MODEL_RCP8.5_IX_5$results$par)-1))-
```

#Delta – new sub-daily data

```
Delta_NEW_MODEL_RCP8.5_5 <- AICc_NEW_MODEL_RCP8.5_5-min(AICc_NEW_MODEL_RCP8.5_5)
```

#LR test – new sub-daily data

```
LR_NEW_MODEL_RCP8.5_5 <- c(lr.test(GEV_NEW_MODEL_RCP8.5_I_5,GEV_NEW_MODEL_RCP8.5_I_5)$p.value,lr.test(GEV_NEW_MODEL_RCP8.5_I_5,GEV_NEW_MODEL_RCP8.5_II_5)$p.value,lr.test(GEV_NEW_MODEL_RCP8.5_I_5,GEV_NEW_MODEL_RCP8.5_III_5)$p.value,lr.test(GEV_NEW_MODEL_RCP8.5_I_5,GEV_NEW_MODEL_RCP8.5_IV_5)$p.value,lr.test(GEV_NEW_MODEL_RCP8.5_I_5,GEV_NEW_MODEL_RCP8.5_V_5)$p.value,lr.test(GEV_NEW_MODEL_RCP8.5_I_5,GEV_NEW_MODEL_RCP8.5_VI_5)$p.value,lr.test(GEV_NEW_MODEL_RCP8.5_I_5,GEV_NEW_MODEL_RCP8.5_VII_5)$p.value,lr.test(GEV_NEW_MODEL_RCP8.5_I_5,GEV_NEW_MODEL_RCP8.5_VIII_5)$p.value,lr.test(GEV_NEW_MODEL_RCP8.5_I_5,GEV_NEW_MODEL_RCP8.5_IX_5)$p.value)
```

- **Return Level Estimation**

Estimate return level based on designated return period (RP)

```
RP <- c(2,5,10,20,25,50,100)
```

#Here the GEV model corresponds to that which has testify as the best one. In this case, GEV model type VII improves 360 minutes new sub-daily data fitting.

```
PTOT_MODEL_RCP8.5_5 <- erlevd(GEV_NEW_MODEL_RCP2.6_VII_360,period = RP)
```

#95th quantiles can be extracted by using the following command:

```
c(quantile(PTOT_MODEL_RCP8.5_5[1,],0.95),quantile(PTOT_MODEL_RCP8.5_5[2,],0.95),quantile(PTOT_MODEL_RCP8.5_5[3,],0.95),quantile(PTOT_MODEL_RCP8.5_5[4,],0.95),quantile(PTOT_MODEL_RCP8.5_5[5,],0.95),quantile(PTOT_MODEL_RCP8.5_5[6,],0.95),quantile(PTOT_MODEL_RCP8.5_5[7,],0.95))
```

- **GCM IDF for future sub-daily**

#Calculate I-d-f for new sub-daily data

```
I_H_5 <- PTOT_MODEL_RCP8.5_5*(60/5)
```

Appendix d: Previous reports in the Series

ISSN: (Print) 1913-3200; (online) 1913-3219
In addition to 78 previous reports (No. 01 – No. 78) prior to 2012

Samiran Das and Slobodan P. Simonovic (2012). Assessment of Uncertainty in Flood Flows under Climate Change. Water Resources Research Report no. 079, Facility for Intelligent Decision Support, Department of Civil and Environmental Engineering, London, Ontario, Canada, 67 pages. ISBN: (print) 978-0-7714-2960-6; (online) 978-0-7714-2961-3.

Rubaiya Sarwar, Sarah E. Irwin, Leanna King and Slobodan P. Simonovic (2012). Assessment of Climatic Vulnerability in the Upper Thames River basin: Downscaling with SDSM. Water Resources Research Report no. 080, Facility for Intelligent Decision Support, Department of Civil and Environmental Engineering, London, Ontario, Canada, 65 pages. ISBN: (print) 978-0-7714-2962-0; (online) 978-0-7714-2963-7.

Sarah E. Irwin, Rubaiya Sarwar, Leanna King and Slobodan P. Simonovic (2012). Assessment of Climatic Vulnerability in the Upper Thames River basin: Downscaling with LARS-WG. Water Resources Research Report no. 081, Facility for Intelligent Decision Support, Department of Civil and Environmental Engineering, London, Ontario, Canada, 80 pages. ISBN: (print) 978-0-7714-2964-4; (online) 978-0-7714-2965-1.

Samiran Das and Slobodan P. Simonovic (2012). Guidelines for Flood Frequency Estimation under Climate Change. Water Resources Research Report no. 082, Facility for Intelligent Decision Support, Department of Civil and Environmental Engineering, London, Ontario, Canada, 44 pages. ISBN: (print) 978-0-7714-2973-6; (online) 978-0-7714-2974-3.

Angela Peck and Slobodan P. Simonovic (2013). Coastal Cities at Risk (CCaR): Generic System Dynamics Simulation Models for Use with City Resilience Simulator. Water Resources Research Report no. 083, Facility for Intelligent Decision Support, Department of Civil and Environmental Engineering, London, Ontario, Canada, 55 pages. ISBN: (print) 978-0-7714-3024-4; (online) 978-0-7714-3025-1.60

Roshan Srivastav and Slobodan P. Simonovic (2014). Generic Framework for Computation of Spatial Dynamic Resilience. Water Resources Research Report no. 085, Facility for Intelligent Decision Support, Department of Civil and Environmental Engineering, London, Ontario, Canada, 81 pages. ISBN: (print) 978-0-7714-3067-1; (online) 978-0-7714-3068-8.

Angela Peck and Slobodan P. Simonovic (2014). Coupling System Dynamics with Geographic Information Systems: CCaR Project Report. Water Resources Research Report no. 086, Facility for Intelligent Decision Support, Department of Civil and Environmental Engineering, London, Ontario, Canada, 60 pages. ISBN: (print) 978-0-7714-3069-5; (online) 978-0-7714-3070-1.

Sarah Irwin, Roshan Srivastav and Slobodan P. Simonovic (2014). Instruction for Watershed Delineation in an ArcGIS Environment for Regionalization Studies.Water Resources Research Report no. 087, Facility for Intelligent Decision Support, Department of Civil and Environmental

Engineering, London, Ontario, Canada, 45 pages. ISBN: (print) 978-0-7714-3071-8; (online) 978-0-7714-3072-5.

Andre Schardong, Roshan K. Srivastav and Slobodan P. Simonovic (2014). Computerized Tool for the Development of Intensity-Duration-Frequency Curves under a Changing Climate: Users Manual v.1. Water Resources Research Report no. 088, Facility for Intelligent Decision Support, Department of Civil and Environmental Engineering, London, Ontario, Canada, 68 pages. ISBN: (print) 978-0-7714-3085-5; (online) 978-0-7714-3086-2.

Roshan K. Srivastav, Andre Schardong and Slobodan P. Simonovic (2014). Computerized Tool for the Development of Intensity-Duration-Frequency Curves under a Changing Climate: Technical Manual v.1. Water Resources Research Report no. 089, Facility for Intelligent Decision Support, Department of Civil and Environmental Engineering, London, Ontario, Canada, 62 pages. ISBN: (print) 978-0-7714-3087-9; (online) 978-0-7714-3088-6.

Roshan K. Srivastav and Slobodan P. Simonovic (2014). Simulation of Dynamic Resilience: A Railway Case Study. Water Resources Research Report no. 090, Facility for Intelligent Decision Support, Department of Civil and Environmental Engineering, London, Ontario, Canada, 91 pages. ISBN: (print) 978-0-7714-3089-3; (online) 978-0-7714-3090-9.61

Nick Agam and Slobodan P. Simonovic (2015). Development of Inundation Maps for the Vancouver Coastline Incorporating the Effects of Sea Level Rise and Extreme Events. Water Resources Research Report no. 091, Facility for Intelligent Decision Support, Department of Civil and Environmental Engineering, London, Ontario, Canada, 107 pages. ISBN: (print) 978-0-7714-3092-3; (online) 978-0-7714-3094-7.

Sarah Irwin, Roshan K. Srivastav and Slobodan P. Simonovic (2015). Instructions for Operating the Proposed Regionalization Tool "Cluster-FCM" Using Fuzzy C-Means Clustering and L-Moment Statistics. Water Resources Research Report no. 092, Facility for Intelligent Decision Support, Department of Civil and Environmental Engineering, London, Ontario, Canada, 54 pages. ISBN: (print) 978-0-7714-3101-2; (online) 978-0-7714-3102-9.

Bogdan Pavlovic and Slobodan P. Simonovic (2016). Automated Control Flaw Generation Procedure: Cheakamus Dam Case Study. Water Resources Research Report no. 093, Facility for Intelligent Decision Support, Department of Civil and Environmental Engineering, London, Ontario, Canada, 78 pages. ISBN: (print) 978-0-7714-3113-5; (online) 978-0-7714-3114-2.

Sarah Irwin, Slobodan P. Simonovic and Niru Nirupama (2016). Introduction to ResilSIM: A Decision Support Tool for Estimating Disaster Resilience to Hydro-Meteorological Events. Water Resources Research Report no. 094, Facility for Intelligent Decision Support, Department of Civil and Environmental Engineering, London, Ontario, Canada, 66 pages. ISBN: (print) 978-0-7714-3115-9; (online) 978-0-7714-3116-6.

Tommy Kokas, Slobodan P. Simonovic (2016). Flood Risk Management in Canadian Urban Environments: A Comprehensive Framework for Water Resources Modeling and Decision-Making. Water Resources Research Report no. 095. Facility for Intelligent Decision Support, Department of Civil and Environmental Engineering, London, Ontario, Canada, 66 pages. ISBN: (print) 978-0-7714-3117-3; (online) 978-0-7714-3118-0.

Jingjing Kong and Slobodan P. Simonovic (2016). Interdependent Infrastructure Network Resilience Model with Joint Restoration Strategy. Water Resources Research Report no. 096, Facility for Intelligent Decision Support, Department of Civil and Environmental Engineering, London, Ontario, Canada, 83 pages. ISBN: (print) 978-0-7714-3132-6; (online) 978-0-7714-3133-3.

Sohom Mandal, Patrick A. Breach and Slobodan P. Simonovic (2017). Tools for Downscaling Climate Variables: A Technical Manual. Water Resources Research Report no. 097, Facility for Intelligent Decision Support, Department of Civil and Environmental Engineering, London, Ontario, Canada, 95 pages. ISBN: (print) 978-0-7714-3135-7; (online) 978-0-7714-3136-4.

Andre Schardong, Abhishek Gaur, Slobodan P. Simonovic and Dan Sandink (2018). Computerized Tool for Development of Intensity-Duration-Frequency Curves Under a Changing Climate: A Technical Manual. Water Resources Research Report no. 103, Facility for Intelligent Decision Support, Department of Civil and Environmental Engineering, London, Ontario, Canada, 67 pages. ISBN: (online) 978-0-7714-3107-4.

Andre Schardong, Slobodan P. Simonovic and Dan Sandink (2018). Computerized Tool for the Development of Intensity-Duration-Frequency Curves Under a Changing Climate: User's Manual v.3. Water Resources Research Report no. 104, Facility for Intelligent Decision Support, Department of Civil and Environmental Engineering, London, Ontario, Canada, 80 pages. ISBN: 978-0-7714-3108-1.

Andre Schardong, Slobodan P. Simonovic and Howard Tong (2018). Use of Quantitative Resilience in Managing Urban Infrastructure Response to Natural Hazards: A Web-Based Decision Support Tool – ResilSIMt. Water Resources Research Report no. 105, Facility for Intelligent Decision Support, Department of Civil and Environmental Engineering, London, Ontario, Canada, 108 pages. ISBN: 978-0-7714-3115-9.